Studying QCD at Finite Density

Prasad Hegde

Center for High Energy Physics,

Indian Institute of Science, Bangalore

4th May 2017

Free Meson Seminar,

Tata Institute of Fundamental Research, Mumbai.

QCD at finite density

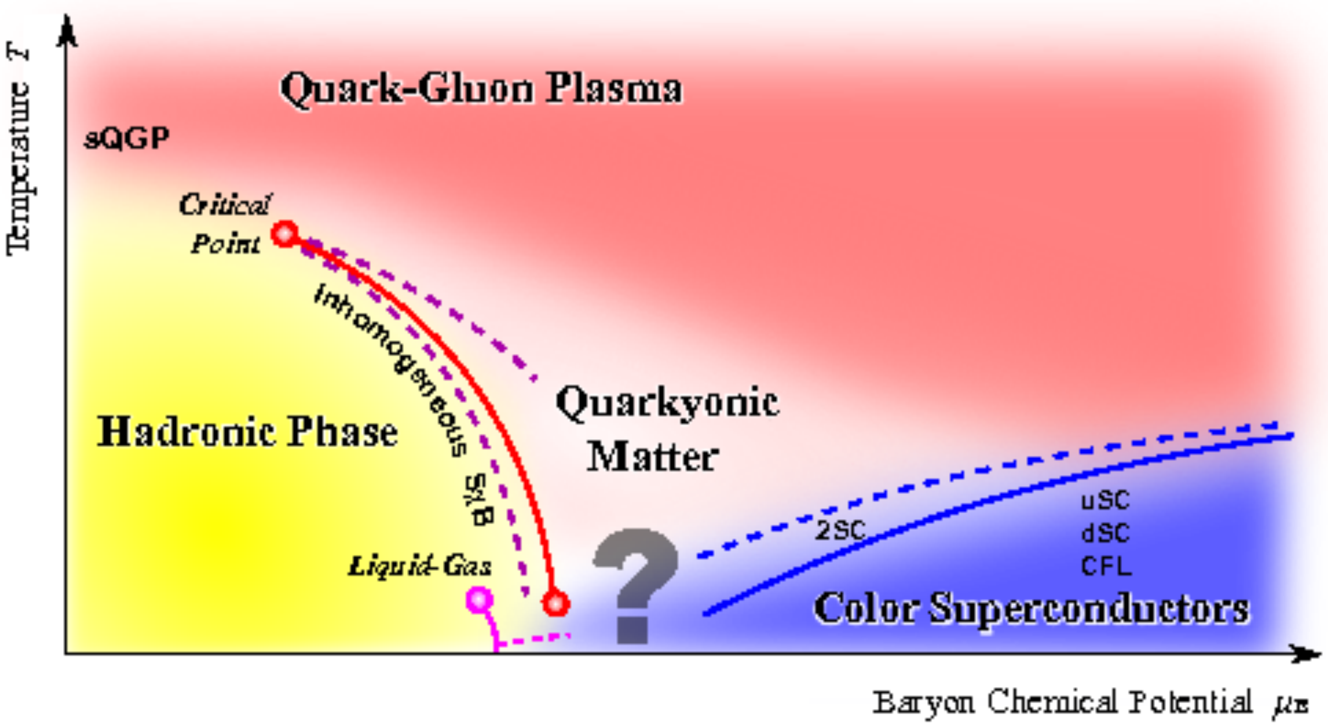

Ordinary nuclear matter: μ_B ~ 940 MeV and T ~ 0K.
Rest of the diagram virtually unknown.

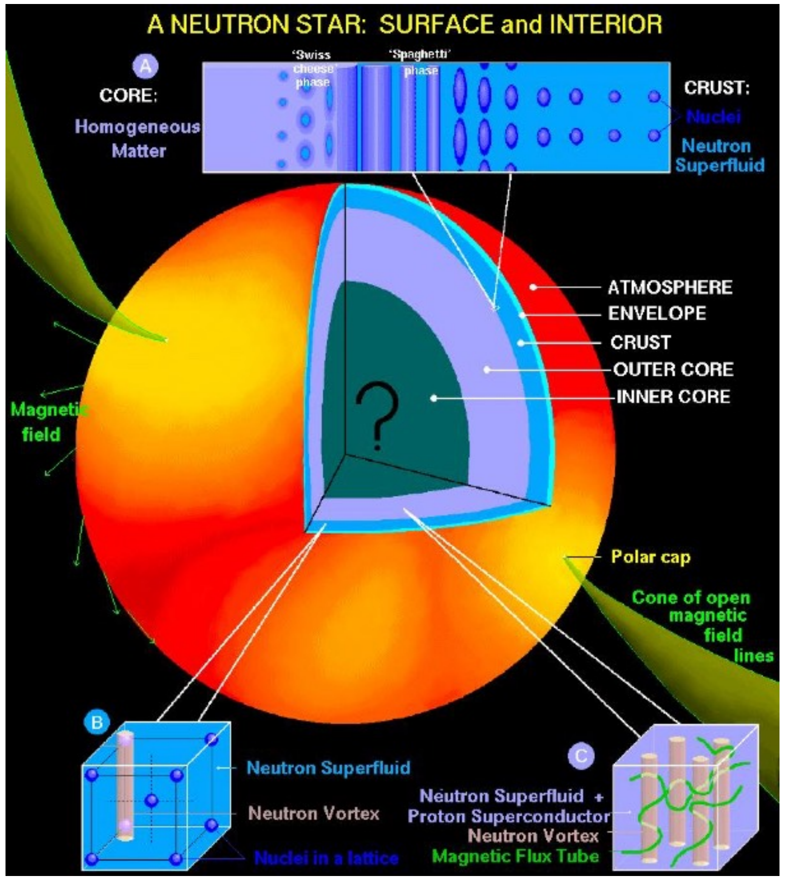

Dense nuclear matter can be found in nature, in the interiors (and surface) of neutron stars for e.g.

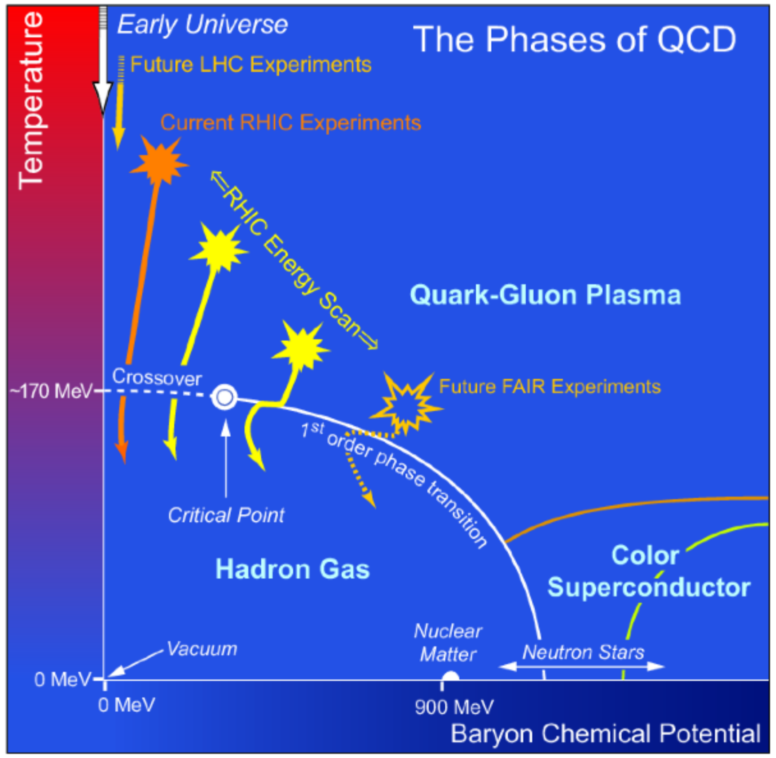

Some parts of this phase diagram will be explored at RHIC, as well as at FAIR, NICA & J-PARC in the future.

Beam Energy Scan and the QCD Critical Point

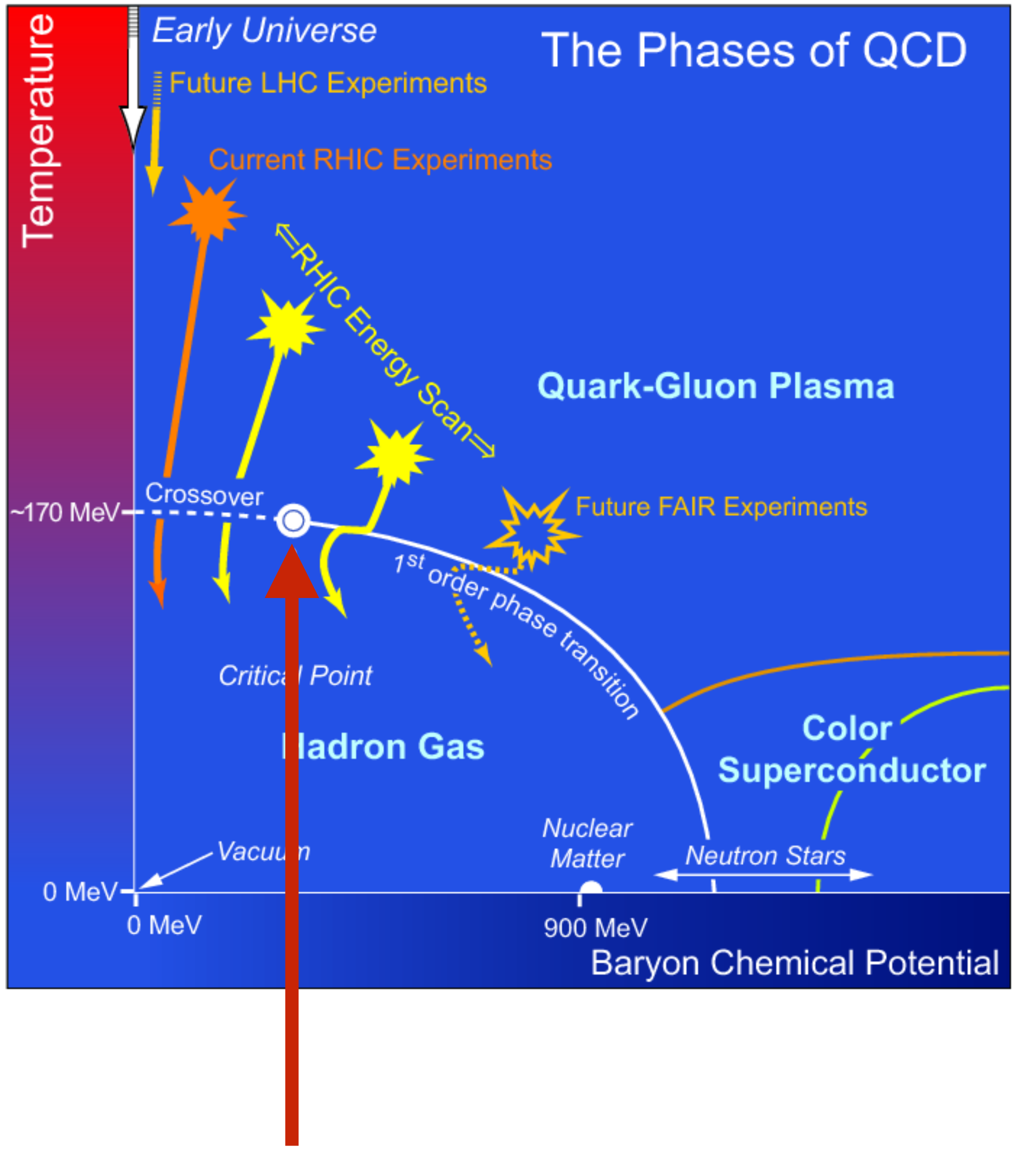

The Beam Energy Scan (BES) program at RHIC was designed to look for the conjectured QCD critical point.

The collision energy of the heavy ions is to be varied from the top RHIC energy of 200A-GeV down to about 5.5A-GeV.

The hadrons formed in a lower energy collision have a higher baryochemical potential μ_B at freezeout.

If a critical point exists, then the evolution of the fireball created in these collisions should be qualitatively different in the first order region than in the crossover region.

Beam Energy Scan and the QCD Critical Point

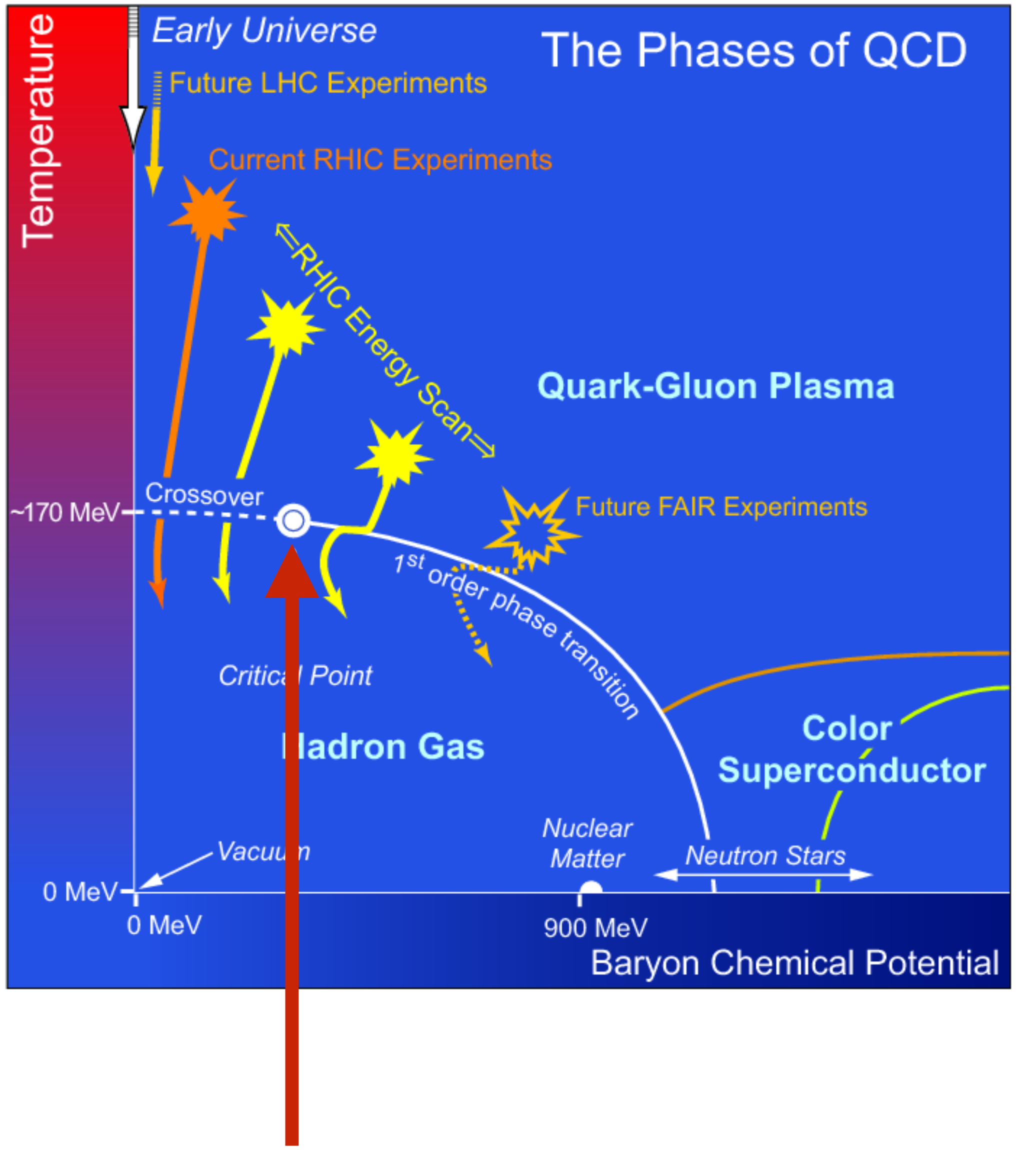

The Beam Energy Scan (BES) program at RHIC was designed to look for the conjectured QCD critical point.

The collision energy of the heavy ions is to be varied from the top RHIC energy of 200A-GeV down to about 5.5A-GeV.

The hadrons formed in a lower energy collision have a higher baryochemical potential μ_B at freezeout.

If a critical point exists, then the evolution of the fireball created in these collisions should be qualitatively different in the first order region than in the crossover region.

Need to validate any experimental observation from theory. Some theoretical estimates place the critical point at μ_B/T ~ 1.5-2 while others place it much higher.

Calculating at finite density

Interesting physics, but how to calculate?

- Models (PNJL, large-N_c, etc.): Possible to calculate the equation of state at large densities e.g. for neutron stars. Also possible to sketch out putative phase diagrams for physical as well as lighter-than-physical quark masses. However, results will necessarily be qualitative or semi-quantitative.

- Lattice QCD: *Ab initio,* but afflicted by the sign problem. Several partial solutions known, but only two have been applied to large-scale QCD simulations:

  - Imaginary-μ: No sign problem at imaginary μ; however an analytic continuation is required back to real μ.

  - Method of Taylor expansions: Straightforward definition. However very expensive: Signal-to-noise ratio falls quickly with increasing order and large volumes.

Calculating with QCD-like theories: Some results

P. Costa *et al.* Europhys. Lett. 86 (2009), 31001.

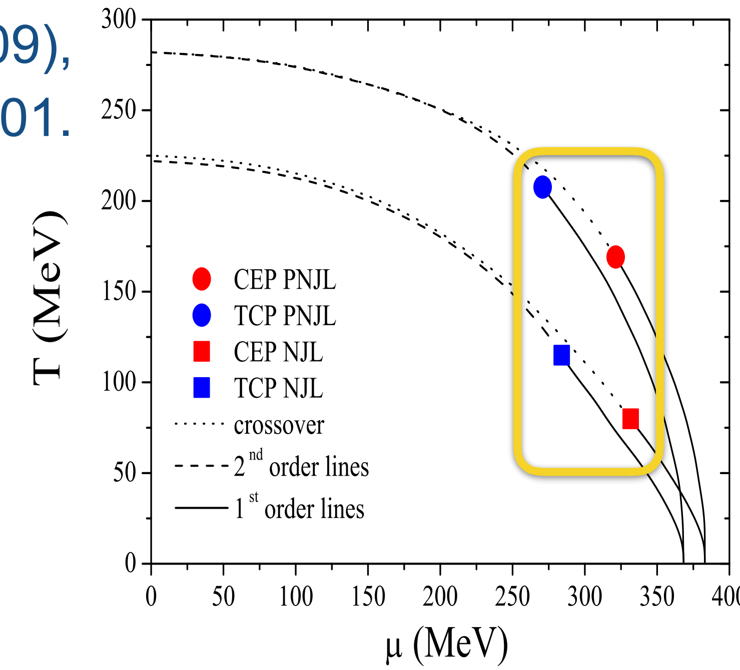

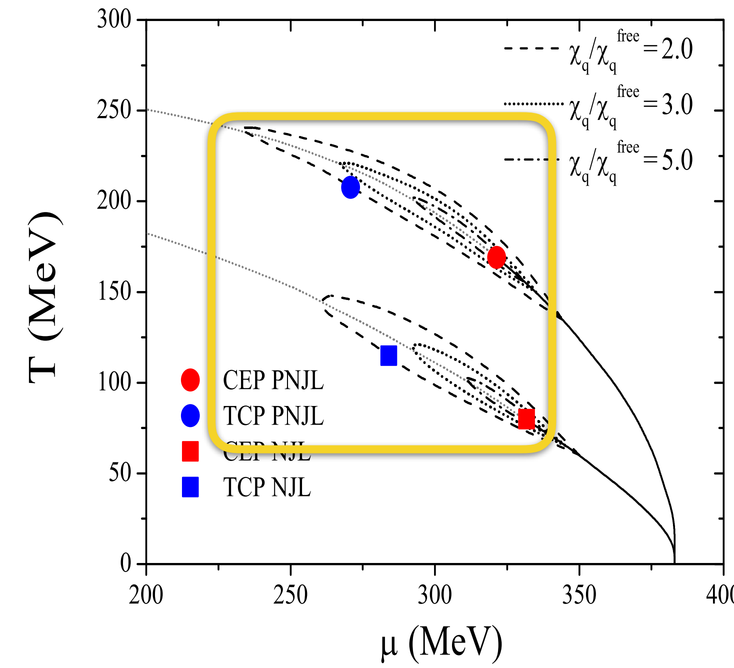

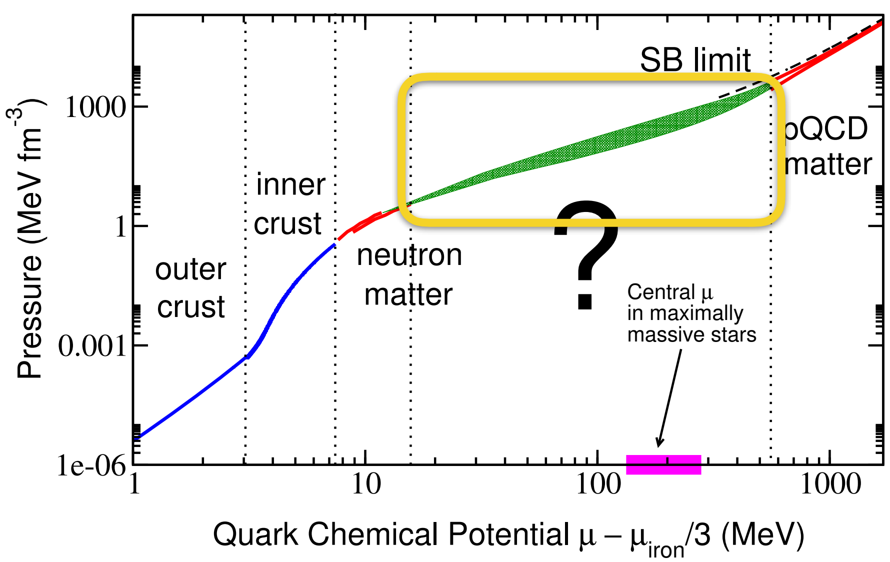

E. Fraga, A. Kurkela and A. Vuorinen, EPJ A52, (2016) no. 3, 49.

T. Kojo, P. Powell, Y. Song and G. Baym, PRD91, no. 4 045003 (2015).

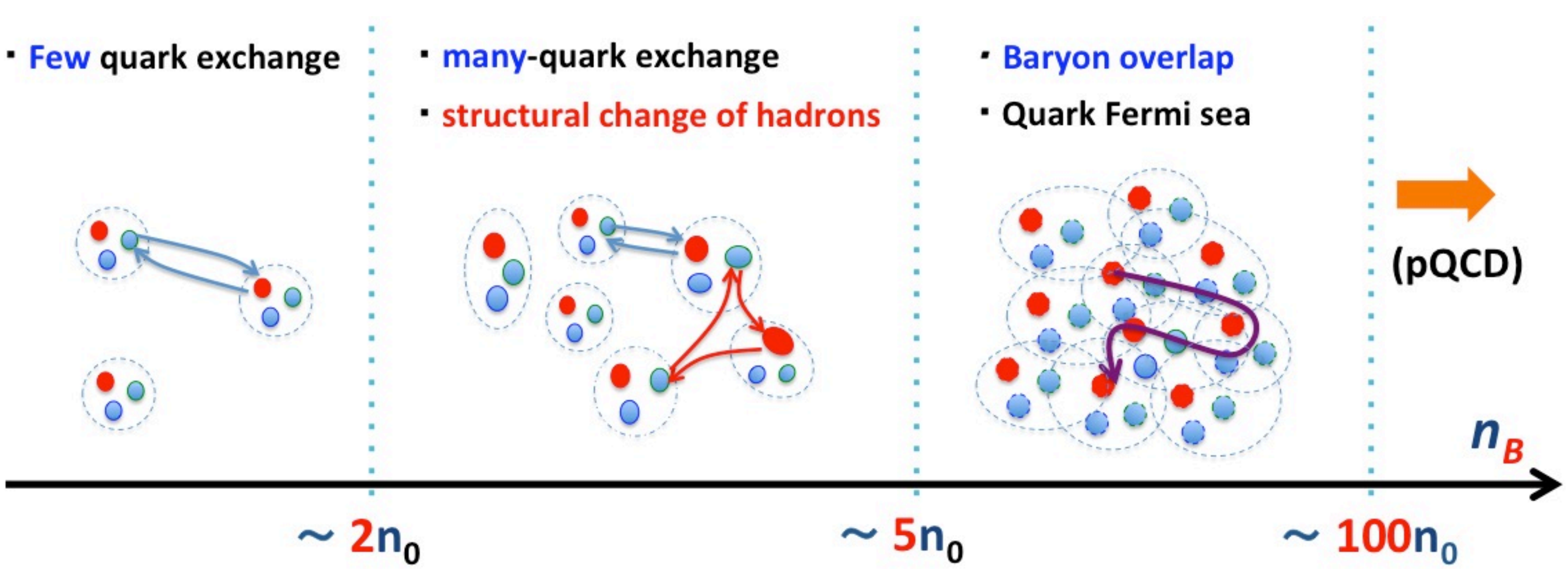

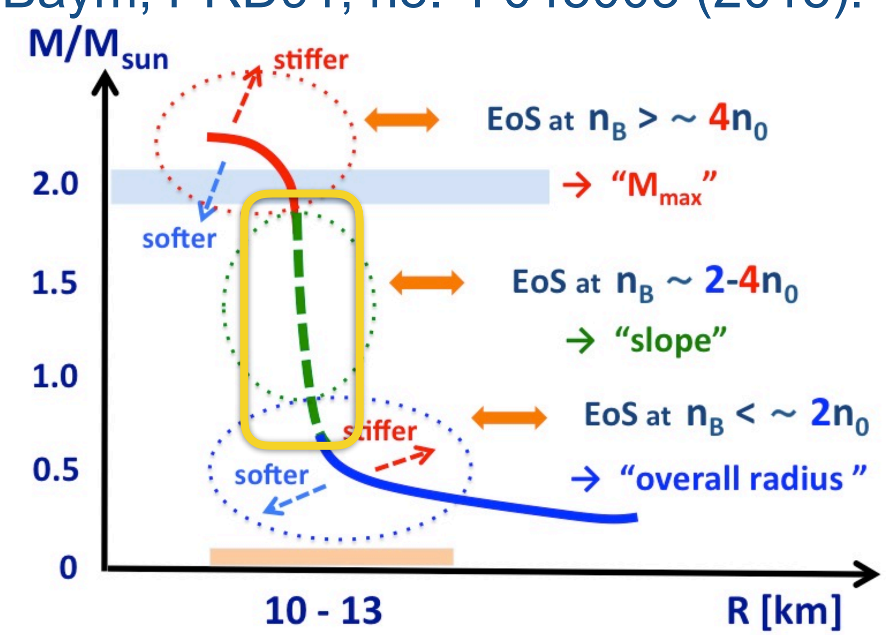

Numerical approaches: Lattice QCD

- Lattice QCD is a first-principles approach to QCD that consists of solving QCD numerically in its difficult non-perturbative regime.

- Although very successful at $T > 0$ and $\mu_B = 0$, it unfortunately suffers from the infamous **sign problem** at μ_B not equal to 0.

- The sign problem occurs when the action becomes complex and the phase can no longer be ignored. Instead of importance sampling i.e. a subset of configurations contributing the most, all configurations now become equally important and the final answer relies on a delicate cancellation of phases.

- No solution to the sign problem is known; however various partial solutions exist of which two viz. analytic continuation and the method of Taylor expansions, have been the most successful.

QCD at imaginary μ

- There is no sign problem at imaginary μ i.e. $\mu = i\mu_i$. Thus one can calculate different observables at various values of $i\mu_i$ and try to analytically continue the results back to real μ.

- It must be kept in mind however that at high values of T, one has the Roberge-Weiss (RW) first order transition at $\mu_i = 2\pi T$. At low temperatures, there are no such restrictions on the allowed values of μ_i.

- Another possible source of systematic error comes from the choice of function used to perform the analytic continuation (polynomial, rational function, etc.).

- In practice however, good results have been obtained by this method, especially for the quark number susceptibilities [M. D'Elia, G. Gagliardi and F. Sanfilippo, arXiv:1611.08285], which we shall discuss next [See also Guenther et al. EPJ Web Conf. 137 (2017) 07008]. Similarly, there are also results for the curvature of the chiral phase transition line [D'Elia *et al*. Wuppertal-Budapest, Cea *et al.* (2015)], which too are in good agreement with results obtained from the Taylor method [Bielefeld-BNL 2009].

QCD at imaginary μ

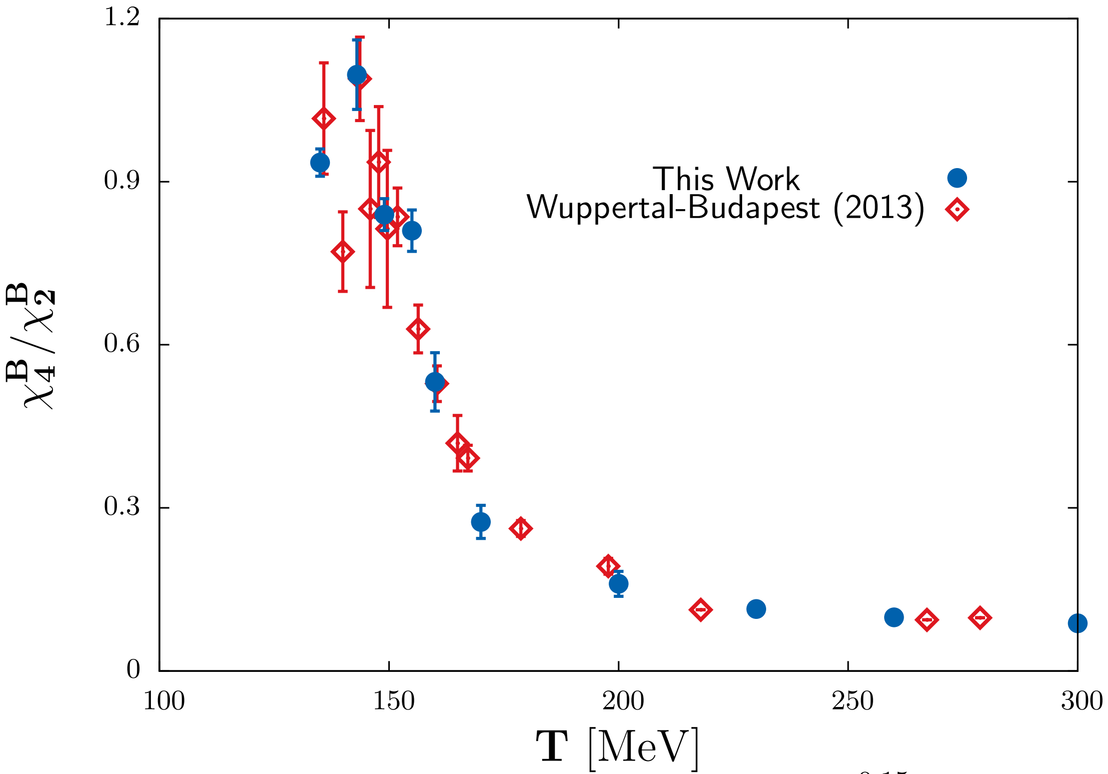

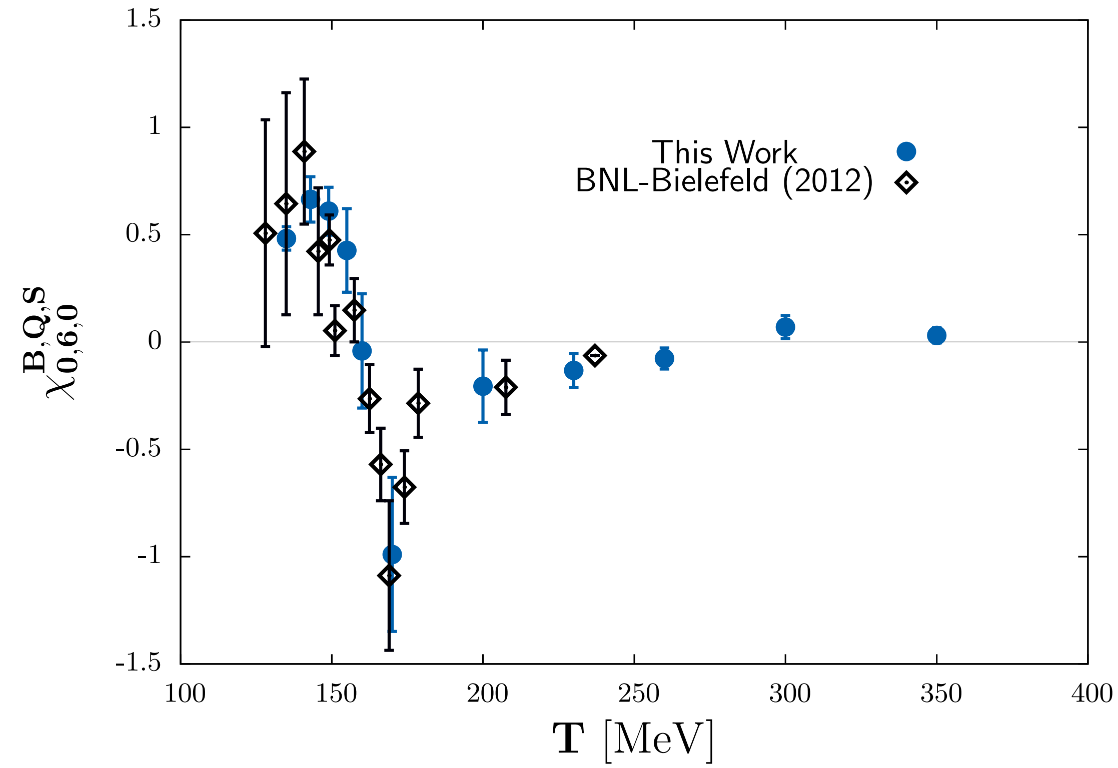

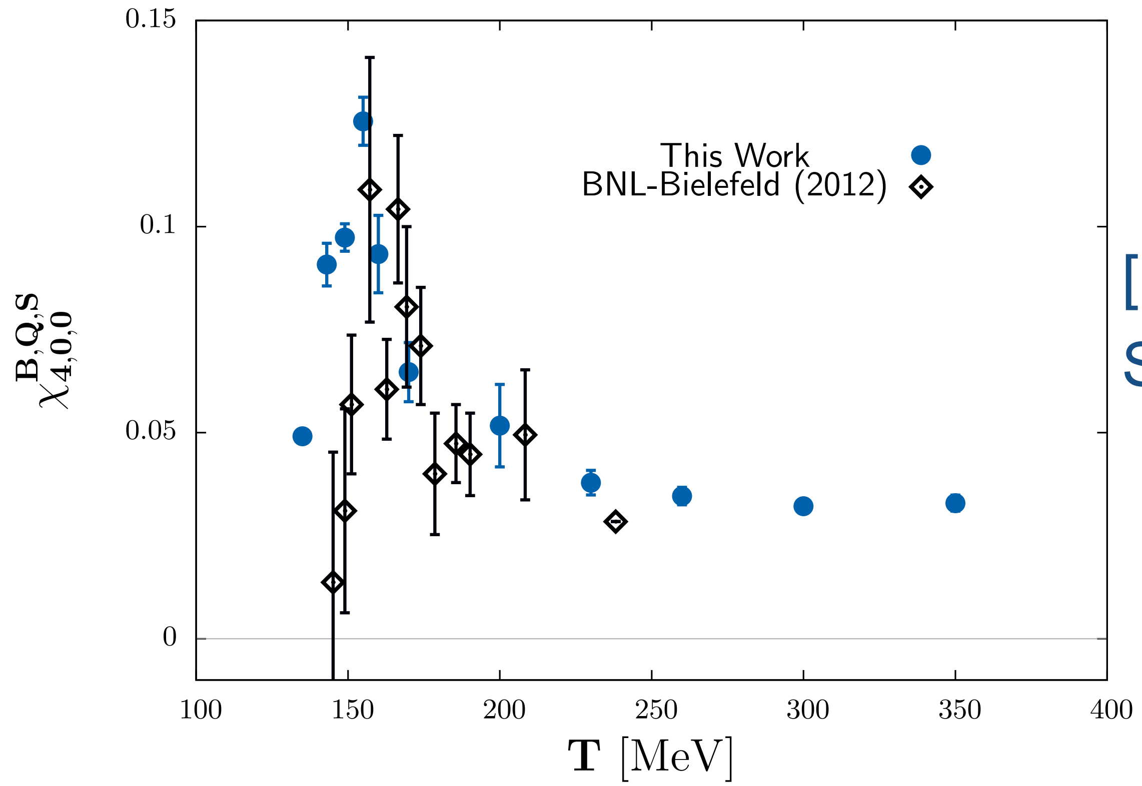

[M. D'Elia, G. Gagliardi and F. Sanfilippo, arXiv:1611.08285].

- Quite good agreement with the Wuppertal-Budapest results, as also with the old (p4) Bielefeld-BNL results.

The method of Taylor expansions

- The quark number susceptibilities (QNS) are the Taylor coefficients of the expansion of the pressure i.e. logarithm of the partition function, w.r.t. the chemical potential μ.

$$\chi_{ijk}^{BQS} = \left[\frac{\partial^{i+j+k}}{\partial \hat{\mu}_B^i \partial \hat{\mu}_Q^j \partial \hat{\mu}_S^k} \left(\frac{p}{T^4} \right) \right]_{\mu_B=\mu_Q=\mu_S=0} \qquad (\hat{\mu} \equiv \mu/T)$$

- To calculate these on the lattice, it is necessary to take derivatives of the quark matrix e.g.

$$\begin{aligned}
\frac{\partial^6 \ln \det M}{\partial \mu^6} = {} & \mathrm{Tr}\left(M^{-1}\frac{\partial^6 M}{\partial \mu^6}\right) - 6\,\mathrm{Tr}\left(M^{-1}\frac{\partial M}{\partial \mu}M^{-1}\frac{\partial^5 M}{\partial \mu^5}\right) - 15\,\mathrm{Tr}\left(M^{-1}\frac{\partial^2 M}{\partial \mu^2}M^{-1}\frac{\partial^4 M}{\partial \mu^4}\right) - 10\,\mathrm{Tr}\left(M^{-1}\frac{\partial^3 M}{\partial \mu^3}M^{-1}\frac{\partial^3 M}{\partial \mu^3}\right) \\
& + 30\,\mathrm{Tr}\left(M^{-1}\frac{\partial M}{\partial \mu}M^{-1}\frac{\partial M}{\partial \mu}M^{-1}\frac{\partial^4 M}{\partial \mu^4}\right) + 60\,\mathrm{Tr}\left(M^{-1}\frac{\partial M}{\partial \mu}M^{-1}\frac{\partial^2 M}{\partial \mu^2}M^{-1}\frac{\partial^3 M}{\partial \mu^3}\right) \\
& + 60\,\mathrm{Tr}\left(M^{-1}\frac{\partial^2 M}{\partial \mu^2}M^{-1}\frac{\partial M}{\partial \mu}M^{-1}\frac{\partial^3 M}{\partial \mu^3}\right) + 30\,\mathrm{Tr}\left(M^{-1}\frac{\partial^2 M}{\partial \mu^2}M^{-1}\frac{\partial^2 M}{\partial \mu^2}M^{-1}\frac{\partial^2 M}{\partial \mu^2}\right) \\
& - 120\,\mathrm{Tr}\left(M^{-1}\frac{\partial M}{\partial \mu}M^{-1}\frac{\partial M}{\partial \mu}M^{-1}\frac{\partial M}{\partial \mu}M^{-1}\frac{\partial^3 M}{\partial \mu^3}\right) - 180\,\mathrm{Tr}\left(M^{-1}\frac{\partial M}{\partial \mu}M^{-1}\frac{\partial M}{\partial \mu}M^{-1}\frac{\partial^2 M}{\partial \mu^2}M^{-1}\frac{\partial^2 M}{\partial \mu^2}\right) \\
& - 90\,\mathrm{Tr}\left(M^{-1}\frac{\partial M}{\partial \mu}M^{-1}\frac{\partial^2 M}{\partial \mu^2}M^{-1}\frac{\partial M}{\partial \mu}M^{-1}\frac{\partial^2 M}{\partial \mu^2}\right) + 360\,\mathrm{Tr}\left(M^{-1}\frac{\partial M}{\partial \mu}M^{-1}\frac{\partial M}{\partial \mu}M^{-1}\frac{\partial M}{\partial \mu}M^{-1}\frac{\partial M}{\partial \mu}M^{-1}\frac{\partial^2 M}{\partial \mu^2}\right) \\
& - 120\,\mathrm{Tr}\left(M^{-1}\frac{\partial M}{\partial \mu}M^{-1}\frac{\partial M}{\partial \mu}M^{-1}\frac{\partial M}{\partial \mu}M^{-1}\frac{\partial M}{\partial \mu}M^{-1}\frac{\partial M}{\partial \mu}M^{-1}\frac{\partial M}{\partial \mu}\right).
\end{aligned}$$

QCD at finite density

- These traces cannot be evaluated exactly, since M^{-1} cannot be evaluated exactly. They must be evaluated stochastically. In our case, we used ~1,500 random vectors per configuration.

- After these traces are evaluated, they are put together in the necessary combination to calculate the relevant QNS's e.g.

$$\begin{aligned}\mathcal{A}_6 = &\langle \mathcal{D}_6 \rangle + 6\langle \mathcal{D}_5 \mathcal{D}_1 \rangle + 15\langle \mathcal{D}_4 \mathcal{D}_2 \rangle + 10\langle \mathcal{D}_3^2 \rangle \\ &+ 15\langle \mathcal{D}_4 \mathcal{D}_1^2 \rangle + 60\langle \mathcal{D}_3 \mathcal{D}_2 \mathcal{D}_1 \rangle + 15\langle \mathcal{D}_2^3 \rangle \\ &+ 20\langle \mathcal{D}_3 \mathcal{D}_1^3 \rangle + 45\langle \mathcal{D}_2^2 \mathcal{D}_1^2 \rangle + 15\langle \mathcal{D}_2 \mathcal{D}_1^4 \rangle + \langle \mathcal{D}_1^6 \rangle.\end{aligned}$$

Here A_6 is the combination required to calculate χ_6. Care must be taken to evaluate the squares, cubes, etc. in an unbiased manner. Once this is done for each configuration, the QNS can be calculated by averaging over the ensemble.

- The signal-to-noise ratio drops quickly with increasing order. Need very high statistics in order to get a decent result for the higher order susceptibilities.

Coupling the chemical potential μ

- Straightforward coupling of μ to the quark matrix leads to μ^2/a^2 divergences [Hasenfratz & Karsch '84].

- Coupling μ exponentially (so that it appears as part of the fourth component of the vector potential) gets rid of these divergences. However now unlike in the continuum, not only the first but all higher derivatives of the quark matrix are also non-zero. The additional terms act like counterterms that serve to cancel the divergence.

- Alternatively, one may couple μ linearly but to the conserved current [Gavai & Sharma (2010)]. Now divergences do arise and need to be subtracted. However these only appear at 2^{nd} and 4^{th} orders. Higher orders are still divergence free.

- Also, since μ is coupled linearly, all derivatives except the first are zero.

Linear vs Exponential μ

- Coupling μ non-linearly gives rise to all possible derivative terms. The number of terms rises rapidly with increasing order.

- For e.g. in the exponential formalism, at sixth order one has the following traces viz.

$$
\begin{aligned}
\frac{\partial^6 \ln \det M}{\partial \mu^6} = {} & \mathrm{Tr}\left(M^{-1}\frac{\partial^6 M}{\partial \mu^6}\right) - 6\,\mathrm{Tr}\left(M^{-1}\frac{\partial M}{\partial \mu}M^{-1}\frac{\partial^5 M}{\partial \mu^5}\right) - 15\,\mathrm{Tr}\left(M^{-1}\frac{\partial^2 M}{\partial \mu^2}M^{-1}\frac{\partial^4 M}{\partial \mu^4}\right) - 10\,\mathrm{Tr}\left(M^{-1}\frac{\partial^3 M}{\partial \mu^3}M^{-1}\frac{\partial^3 M}{\partial \mu^3}\right) \\
& + 30\,\mathrm{Tr}\left(M^{-1}\frac{\partial M}{\partial \mu}M^{-1}\frac{\partial M}{\partial \mu}M^{-1}\frac{\partial^4 M}{\partial \mu^4}\right) + 60\,\mathrm{Tr}\left(M^{-1}\frac{\partial M}{\partial \mu}M^{-1}\frac{\partial^2 M}{\partial \mu^2}M^{-1}\frac{\partial^3 M}{\partial \mu^3}\right) \\
& + 60\,\mathrm{Tr}\left(M^{-1}\frac{\partial^2 M}{\partial \mu^2}M^{-1}\frac{\partial M}{\partial \mu}M^{-1}\frac{\partial^3 M}{\partial \mu^3}\right) + 30\,\mathrm{Tr}\left(M^{-1}\frac{\partial^2 M}{\partial \mu^2}M^{-1}\frac{\partial^2 M}{\partial \mu^2}M^{-1}\frac{\partial^2 M}{\partial \mu^2}\right) \\
& - 120\,\mathrm{Tr}\left(M^{-1}\frac{\partial M}{\partial \mu}M^{-1}\frac{\partial M}{\partial \mu}M^{-1}\frac{\partial M}{\partial \mu}M^{-1}\frac{\partial^3 M}{\partial \mu^3}\right) - 180\,\mathrm{Tr}\left(M^{-1}\frac{\partial M}{\partial \mu}M^{-1}\frac{\partial M}{\partial \mu}M^{-1}\frac{\partial^2 M}{\partial \mu^2}M^{-1}\frac{\partial^2 M}{\partial \mu^2}\right) \\
& - 90\,\mathrm{Tr}\left(M^{-1}\frac{\partial M}{\partial \mu}M^{-1}\frac{\partial^2 M}{\partial \mu^2}M^{-1}\frac{\partial M}{\partial \mu}M^{-1}\frac{\partial^2 M}{\partial \mu^2}\right) + 360\,\mathrm{Tr}\left(M^{-1}\frac{\partial M}{\partial \mu}M^{-1}\frac{\partial M}{\partial \mu}M^{-1}\frac{\partial M}{\partial \mu}M^{-1}\frac{\partial M}{\partial \mu}M^{-1}\frac{\partial^2 M}{\partial \mu^2}\right) \\
& - 120\,\mathrm{Tr}\left(M^{-1}\frac{\partial M}{\partial \mu}M^{-1}\frac{\partial M}{\partial \mu}M^{-1}\frac{\partial M}{\partial \mu}M^{-1}\frac{\partial M}{\partial \mu}M^{-1}\frac{\partial M}{\partial \mu}M^{-1}\frac{\partial M}{\partial \mu}\right).
\end{aligned}
$$

Linear vs Exponential μ

- Coupling μ non-linearly gives rise to all possible derivative terms. The number of terms rises rapidly with increasing order.

- By contrast, if μ is coupled linearly, all terms with second and higher derivatives of μ are zero.

$$
\begin{aligned}
\frac{\partial^6 \ln \det M}{\partial \mu^6} =\; & \mathrm{Tr}\left(M^{-1}\frac{\partial^6 M}{\partial \mu^6}\right) - 6\,\mathrm{Tr}\left(M^{-1}\frac{\partial M}{\partial \mu}M^{-1}\frac{\partial^5 M}{\partial \mu^5}\right) - 15\,\mathrm{Tr}\left(M^{-1}\frac{\partial^2 M}{\partial \mu^2}M^{-1}\frac{\partial^4 M}{\partial \mu^4}\right) - 10\,\mathrm{Tr}\left(M^{-1}\frac{\partial^3 M}{\partial \mu^3}M^{-1}\frac{\partial^3 M}{\partial \mu^3}\right) \\
& + 30\,\mathrm{Tr}\left(M^{-1}\frac{\partial M}{\partial \mu}M^{-1}\frac{\partial M}{\partial \mu}M^{-1}\frac{\partial^4 M}{\partial \mu^4}\right) + 60\,\mathrm{Tr}\left(M^{-1}\frac{\partial M}{\partial \mu}M^{-1}\frac{\partial^2 M}{\partial \mu^2}M^{-1}\frac{\partial^3 M}{\partial \mu^3}\right) \\
& + 60\,\mathrm{Tr}\left(M^{-1}\frac{\partial^2 M}{\partial \mu^2}M^{-1}\frac{\partial M}{\partial \mu}M^{-1}\frac{\partial^3 M}{\partial \mu^3}\right) + 30\,\mathrm{Tr}\left(M^{-1}\frac{\partial^2 M}{\partial \mu^2}M^{-1}\frac{\partial^2 M}{\partial \mu^2}M^{-1}\frac{\partial^2 M}{\partial \mu^2}\right) \\
& - 120\,\mathrm{Tr}\left(M^{-1}\frac{\partial M}{\partial \mu}M^{-1}\frac{\partial M}{\partial \mu}M^{-1}\frac{\partial M}{\partial \mu}M^{-1}\frac{\partial^3 M}{\partial \mu^3}\right) - 180\,\mathrm{Tr}\left(M^{-1}\frac{\partial M}{\partial \mu}M^{-1}\frac{\partial M}{\partial \mu}M^{-1}\frac{\partial^2 M}{\partial \mu^2}M^{-1}\frac{\partial^2 M}{\partial \mu^2}\right) \\
& - 90\,\mathrm{Tr}\left(M^{-1}\frac{\partial M}{\partial \mu}M^{-1}\frac{\partial^2 M}{\partial \mu^2}M^{-1}\frac{\partial M}{\partial \mu}M^{-1}\frac{\partial^2 M}{\partial \mu^2}\right) + 360\,\mathrm{Tr}\left(M^{-1}\frac{\partial M}{\partial \mu}M^{-1}\frac{\partial M}{\partial \mu}M^{-1}\frac{\partial M}{\partial \mu}M^{-1}\frac{\partial M}{\partial \mu}M^{-1}\frac{\partial^2 M}{\partial \mu^2}\right) \\
& - 120\,\mathrm{Tr}\left(M^{-1}\frac{\partial M}{\partial \mu}M^{-1}\frac{\partial M}{\partial \mu}M^{-1}\frac{\partial M}{\partial \mu}M^{-1}\frac{\partial M}{\partial \mu}M^{-1}\frac{\partial M}{\partial \mu}M^{-1}\frac{\partial M}{\partial \mu}\right).
\end{aligned}
$$

Linear vs Exponential μ

- Coupling μ non-linearly gives rise to all possible derivative terms. The number of terms rises rapidly with increasing order.
- By contrast, if μ is coupled linearly, all terms with second and higher derivatives of μ are zero.

$$
\begin{aligned}
\frac{\partial^6 \ln \det M}{\partial \mu^6} = {} & \mathrm{Tr}\left(M^{-1}\frac{\partial^6 M}{\partial \mu^6}\right) - 6\,\mathrm{Tr}\left(M^{-1}\frac{\partial M}{\partial \mu}M^{-1}\frac{\partial^5 M}{\partial \mu^5}\right) - 15\,\mathrm{Tr}\left(M^{-1}\frac{\partial^2 M}{\partial \mu^2}M^{-1}\frac{\partial^4 M}{\partial \mu^4}\right) - 10\,\mathrm{Tr}\left(M^{-1}\frac{\partial^3 M}{\partial \mu^3}M^{-1}\frac{\partial^3 M}{\partial \mu^3}\right) \\
& + 30\,\mathrm{Tr}\left(M^{-1}\frac{\partial M}{\partial \mu}M^{-1}\frac{\partial M}{\partial \mu}M^{-1}\frac{\partial^4 M}{\partial \mu^4}\right) + 60\,\mathrm{Tr}\left(M^{-1}\frac{\partial M}{\partial \mu}M^{-1}\frac{\partial^2 M}{\partial \mu^2}M^{-1}\frac{\partial^3 M}{\partial \mu^3}\right) \\
& + 60\,\mathrm{Tr}\left(M^{-1}\frac{\partial^2 M}{\partial \mu^2}M^{-1}\frac{\partial M}{\partial \mu}M^{-1}\frac{\partial^3 M}{\partial \mu^3}\right) + 30\,\mathrm{Tr}\left(M^{-1}\frac{\partial^2 M}{\partial \mu^2}M^{-1}\frac{\partial^2 M}{\partial \mu^2}M^{-1}\frac{\partial^2 M}{\partial \mu^2}\right) \\
& - 120\,\mathrm{Tr}\left(M^{-1}\frac{\partial M}{\partial \mu}M^{-1}\frac{\partial M}{\partial \mu}M^{-1}\frac{\partial M}{\partial \mu}M^{-1}\frac{\partial^3 M}{\partial \mu^3}\right) - 180\,\mathrm{Tr}\left(M^{-1}\frac{\partial M}{\partial \mu}M^{-1}\frac{\partial M}{\partial \mu}M^{-1}\frac{\partial^2 M}{\partial \mu^2}M^{-1}\frac{\partial^2 M}{\partial \mu^2}\right) \\
& - 90\,\mathrm{Tr}\left(M^{-1}\frac{\partial M}{\partial \mu}M^{-1}\frac{\partial^2 M}{\partial \mu^2}M^{-1}\frac{\partial M}{\partial \mu}M^{-1}\frac{\partial^2 M}{\partial \mu^2}\right) + 360\,\mathrm{Tr}\left(M^{-1}\frac{\partial M}{\partial \mu}M^{-1}\frac{\partial M}{\partial \mu}M^{-1}\frac{\partial M}{\partial \mu}M^{-1}\frac{\partial M}{\partial \mu}M^{-1}\frac{\partial^2 M}{\partial \mu^2}\right) \\
& \boxed{- 120\,\mathrm{Tr}\left(M^{-1}\frac{\partial M}{\partial \mu}M^{-1}\frac{\partial M}{\partial \mu}M^{-1}\frac{\partial M}{\partial \mu}M^{-1}\frac{\partial M}{\partial \mu}M^{-1}\frac{\partial M}{\partial \mu}M^{-1}\frac{\partial M}{\partial \mu}\right)}.
\end{aligned}
$$

Linear vs Exponential μ

- Thus one only needs N matrix inversions at N^{th} order. By comparison, in the exponential case one needs around 20 matrix inversions at sixth order.
- Since matrix inversion is the most expensive part of the calculation, this results in a huge gain at higher orders.

$$
\begin{aligned}
\frac{\partial^6 \ln \det M}{\partial \mu^6} = {} & \mathrm{Tr}\left(M^{-1}\frac{\partial^6 M}{\partial \mu^6}\right) - 6\,\mathrm{Tr}\left(M^{-1}\frac{\partial M}{\partial \mu}M^{-1}\frac{\partial^5 M}{\partial \mu^5}\right) - 15\,\mathrm{Tr}\left(M^{-1}\frac{\partial^2 M}{\partial \mu^2}M^{-1}\frac{\partial^4 M}{\partial \mu^4}\right) - 10\,\mathrm{Tr}\left(M^{-1}\frac{\partial^3 M}{\partial \mu^3}M^{-1}\frac{\partial^3 M}{\partial \mu^3}\right) \\
& + 30\,\mathrm{Tr}\left(M^{-1}\frac{\partial M}{\partial \mu}M^{-1}\frac{\partial M}{\partial \mu}M^{-1}\frac{\partial^4 M}{\partial \mu^4}\right) + 60\,\mathrm{Tr}\left(M^{-1}\frac{\partial M}{\partial \mu}M^{-1}\frac{\partial^2 M}{\partial \mu^2}M^{-1}\frac{\partial^3 M}{\partial \mu^3}\right) \\
& + 60\,\mathrm{Tr}\left(M^{-1}\frac{\partial^2 M}{\partial \mu^2}M^{-1}\frac{\partial M}{\partial \mu}M^{-1}\frac{\partial^3 M}{\partial \mu^3}\right) + 30\,\mathrm{Tr}\left(M^{-1}\frac{\partial^2 M}{\partial \mu^2}M^{-1}\frac{\partial^2 M}{\partial \mu^2}M^{-1}\frac{\partial^2 M}{\partial \mu^2}\right) \\
& - 120\,\mathrm{Tr}\left(M^{-1}\frac{\partial M}{\partial \mu}M^{-1}\frac{\partial M}{\partial \mu}M^{-1}\frac{\partial M}{\partial \mu}M^{-1}\frac{\partial^3 M}{\partial \mu^3}\right) - 180\,\mathrm{Tr}\left(M^{-1}\frac{\partial M}{\partial \mu}M^{-1}\frac{\partial M}{\partial \mu}M^{-1}\frac{\partial^2 M}{\partial \mu^2}M^{-1}\frac{\partial^2 M}{\partial \mu^2}\right) \\
& - 90\,\mathrm{Tr}\left(M^{-1}\frac{\partial M}{\partial \mu}M^{-1}\frac{\partial^2 M}{\partial \mu^2}M^{-1}\frac{\partial M}{\partial \mu}M^{-1}\frac{\partial^2 M}{\partial \mu^2}\right) + 360\,\mathrm{Tr}\left(M^{-1}\frac{\partial M}{\partial \mu}M^{-1}\frac{\partial M}{\partial \mu}M^{-1}\frac{\partial M}{\partial \mu}M^{-1}\frac{\partial M}{\partial \mu}M^{-1}\frac{\partial^2 M}{\partial \mu^2}\right) \\
& \boxed{- 120\,\mathrm{Tr}\left(M^{-1}\frac{\partial M}{\partial \mu}M^{-1}\frac{\partial M}{\partial \mu}M^{-1}\frac{\partial M}{\partial \mu}M^{-1}\frac{\partial M}{\partial \mu}M^{-1}\frac{\partial M}{\partial \mu}M^{-1}\frac{\partial M}{\partial \mu}\right)}.
\end{aligned}
$$

QCD at finite density

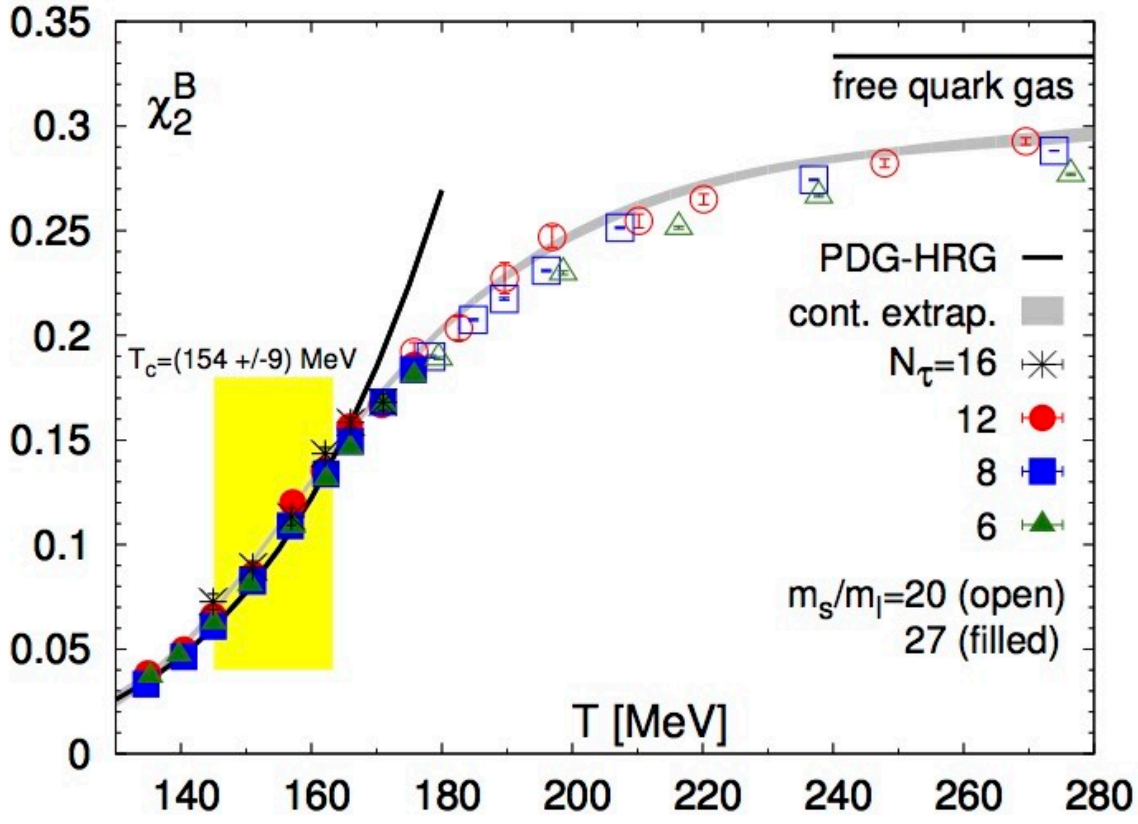

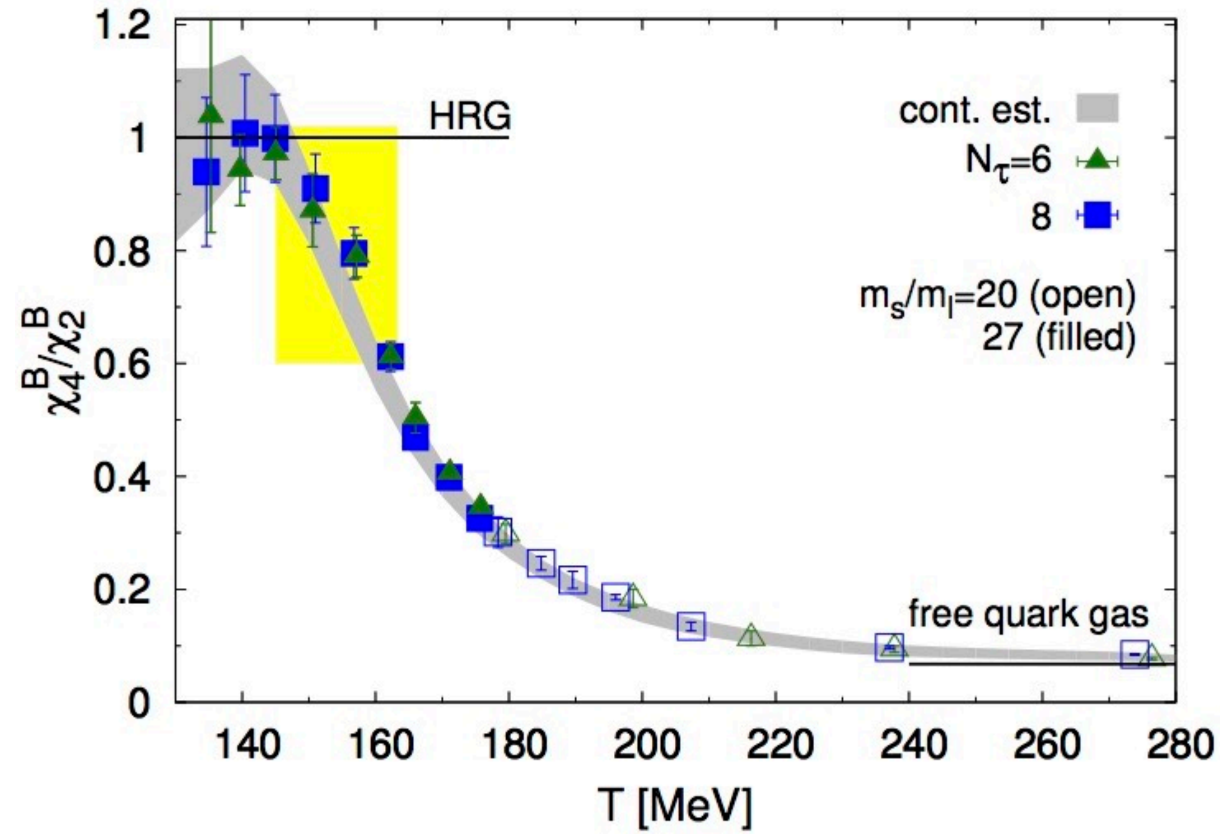

- We calculated all the QNS (49 in all) up to sixth order, on lattices of size 6 – 16, in the temperature range [135 MeV, 280 MeV] and for two quark masses viz. $m_l = m_s/20$ and $m_l = m_s/27$.
- Multiple lattice spacings allowed us to take the continuum limit in the 2nd order case while for the 4th and 6th order cases, our high-statistics results for N_t = 6 & 8 allowed us to calculate the continuum estimate.

QCD at finite density

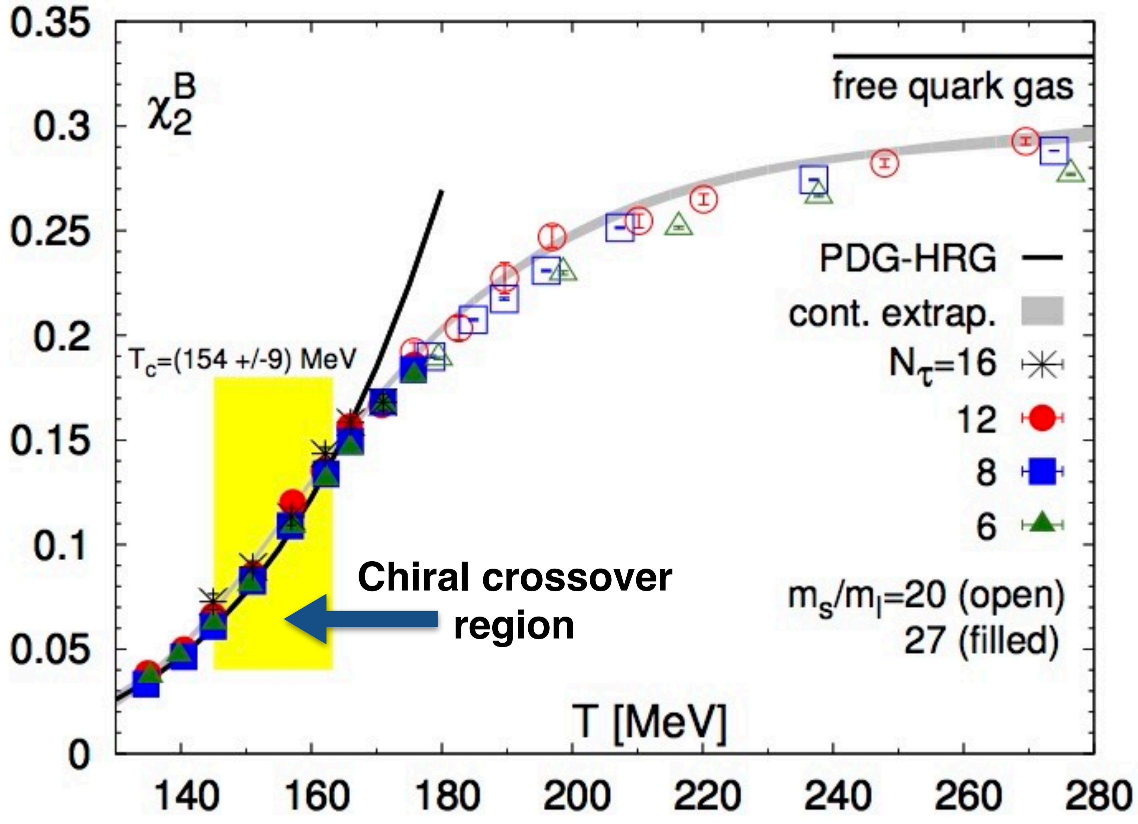

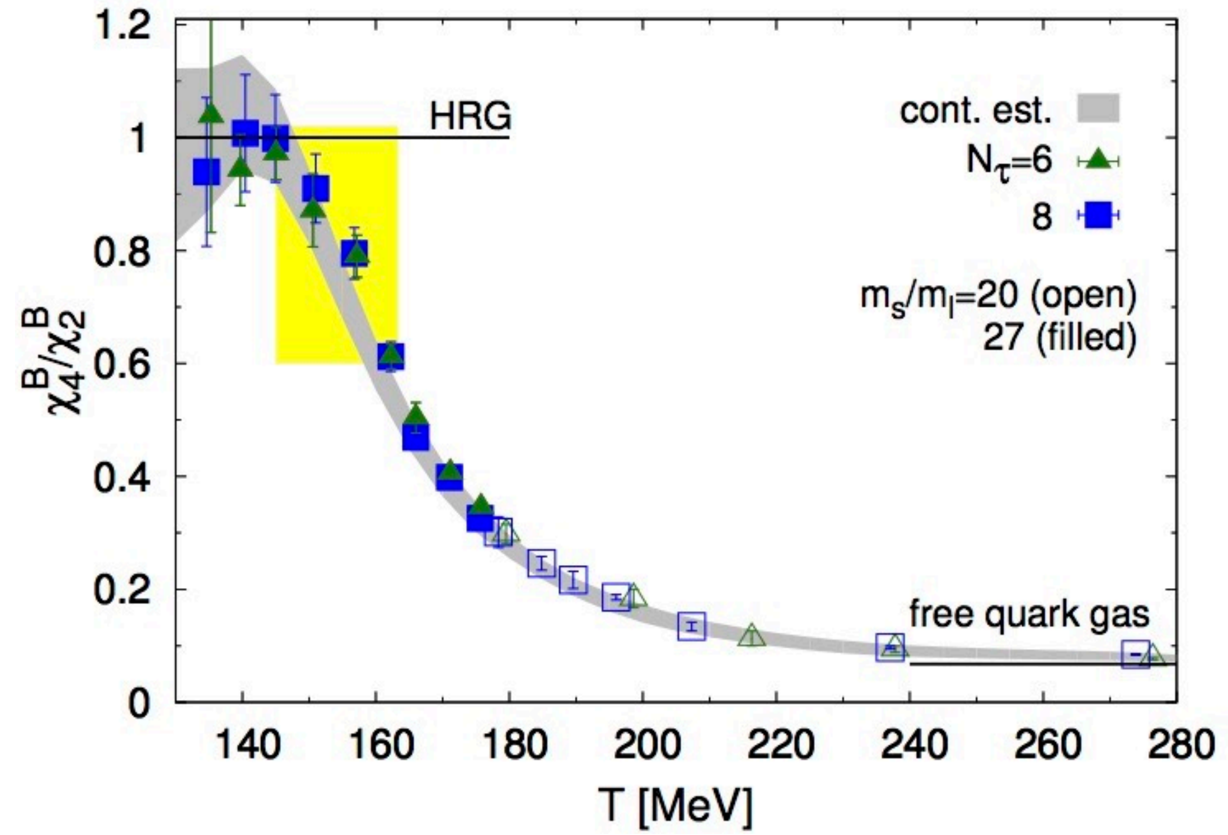

- We used the exponential formalism to calculate 2nd and 4th order QNS, and the linear formalism from the 6th order onwards.
- Our measurements were carried out on 50-100,000 configurations for each temperature, with up to 1,500 random sources on each configuration.

QNS and freezeout parameters

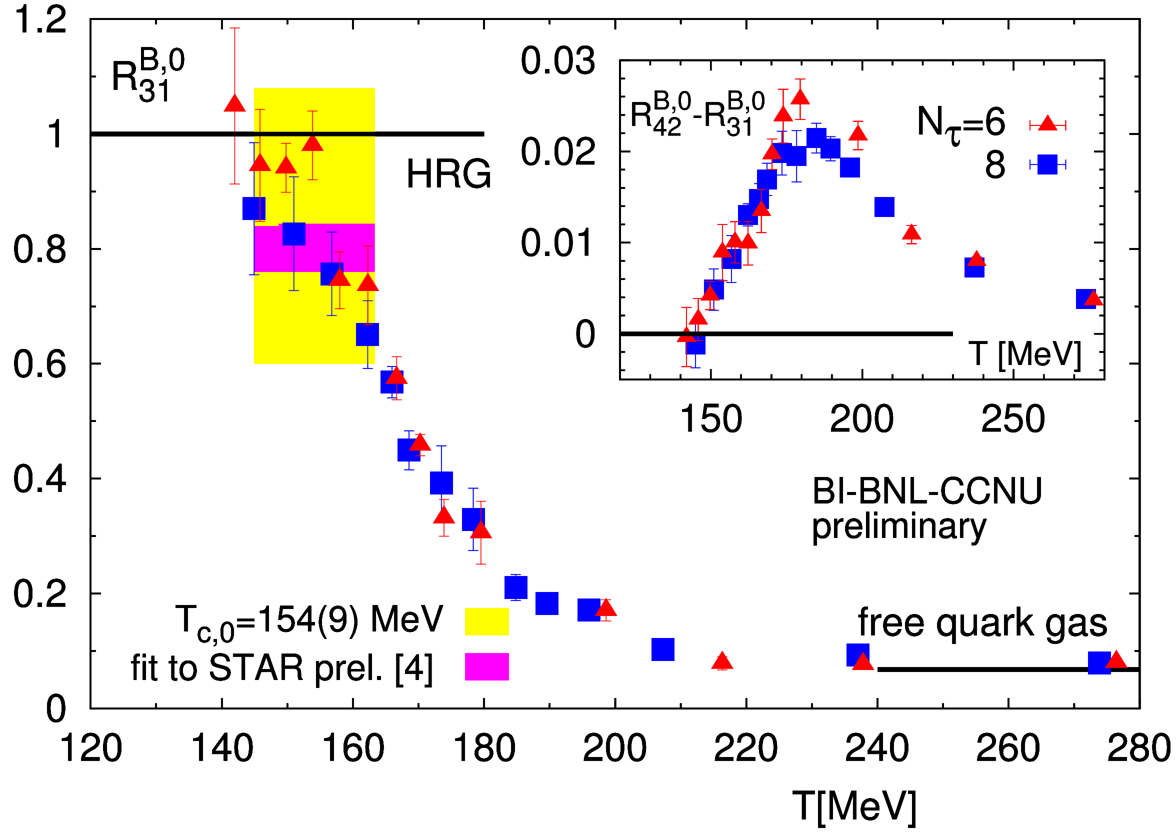

Ratios of QNS can be related to ratios of fluctuations of conserved charges observed experimentally. From a comparison between lattice results and expt. it is possible to extract a value (T^f, $\mu_B{}^f$) at freezeout. This value agrees well with other determinations [F. Karsch, QM2015].

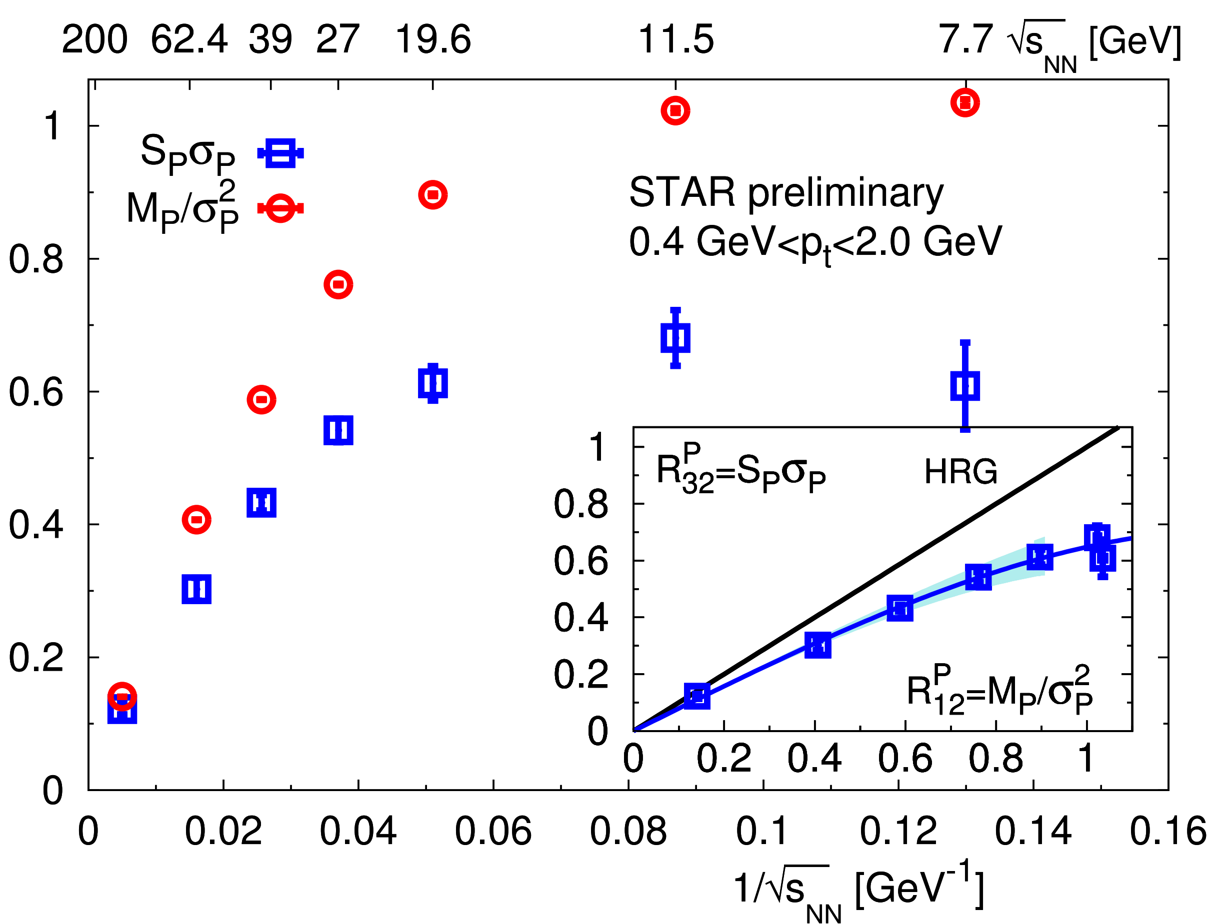

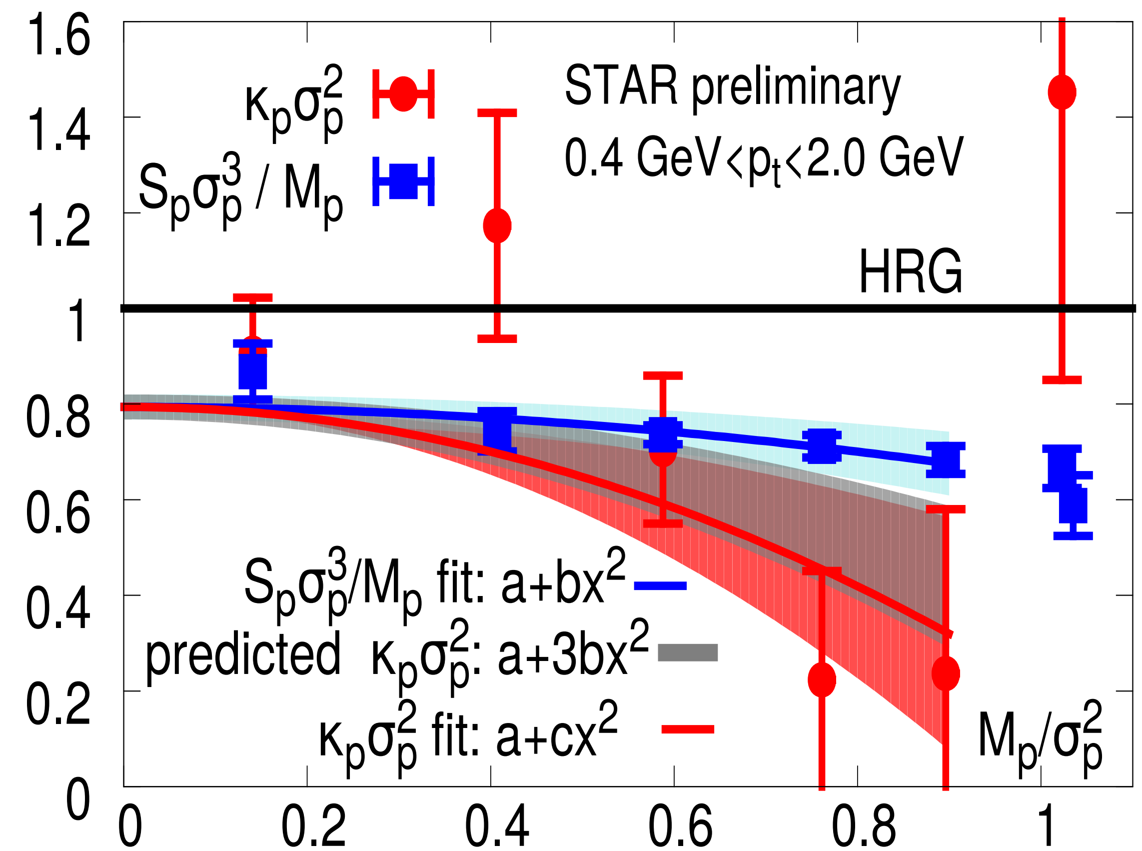

Strangeness neutrality and initial conditions in heavy-ion collisions

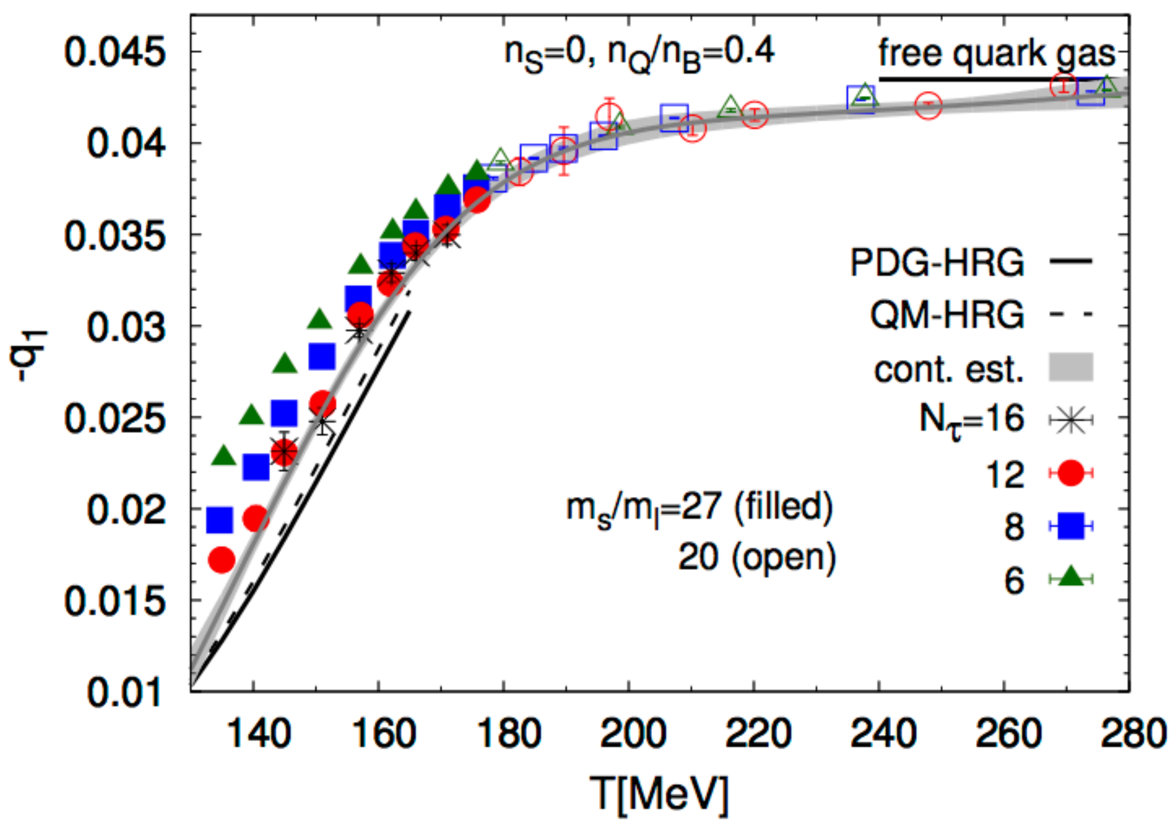

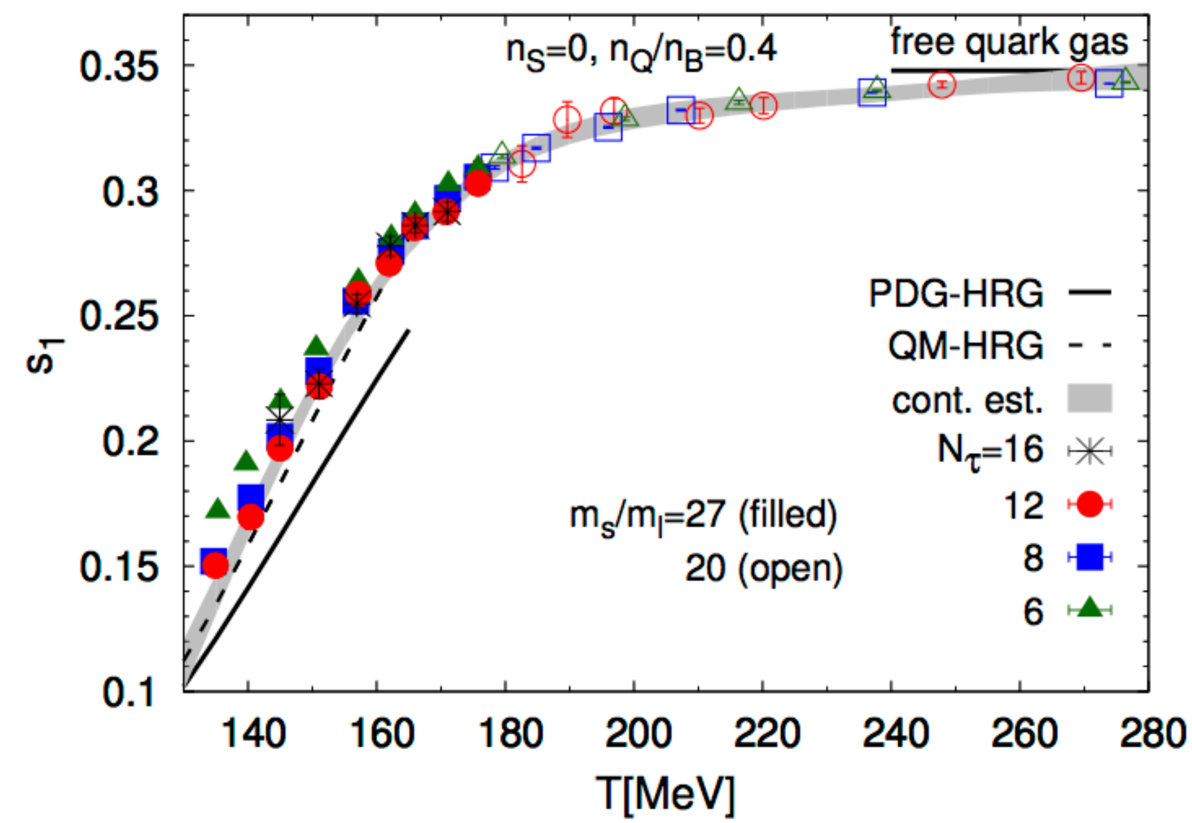

The initial conditions in a heavy-ion collision are i) $n_S = 0$ (net strangeness zero), and ii) $n_Q/n_B = \text{const.}$ (fixed proton-to-neutron ratio).

These conditions imply that μ_Q and μ_S are nonzero whenever μ_B is. Using the QNS, they can be determined order-by-order in μ_B.

Corrections to the pressure

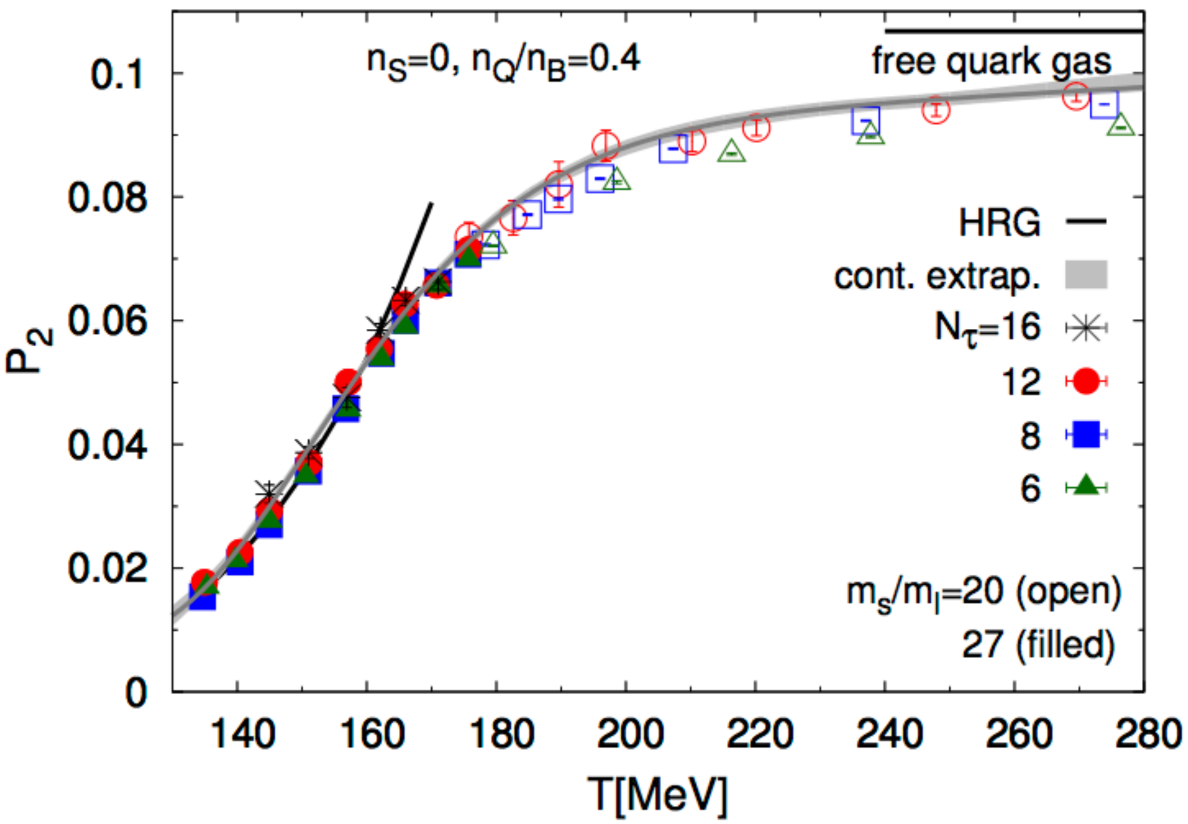

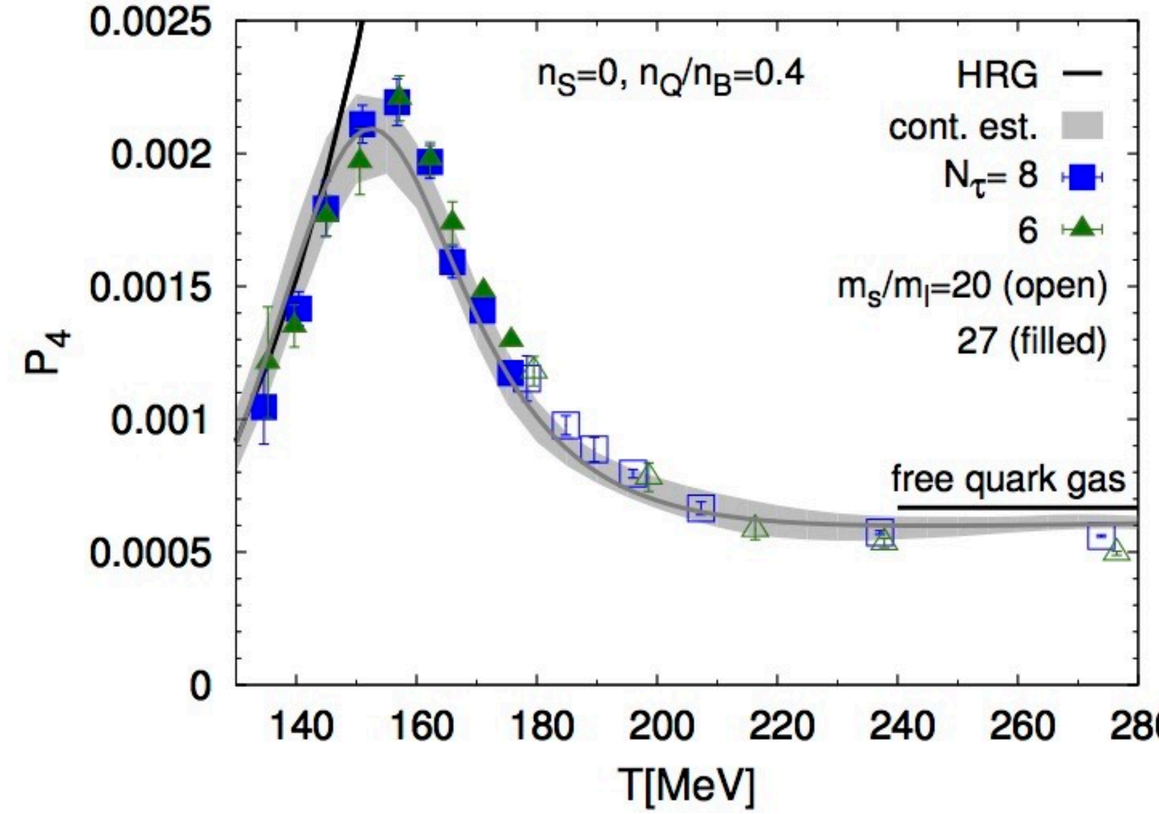

Similar to corrections for the case $\mu_Q = \mu_S = 0$ but about 20% smaller in magnitude.

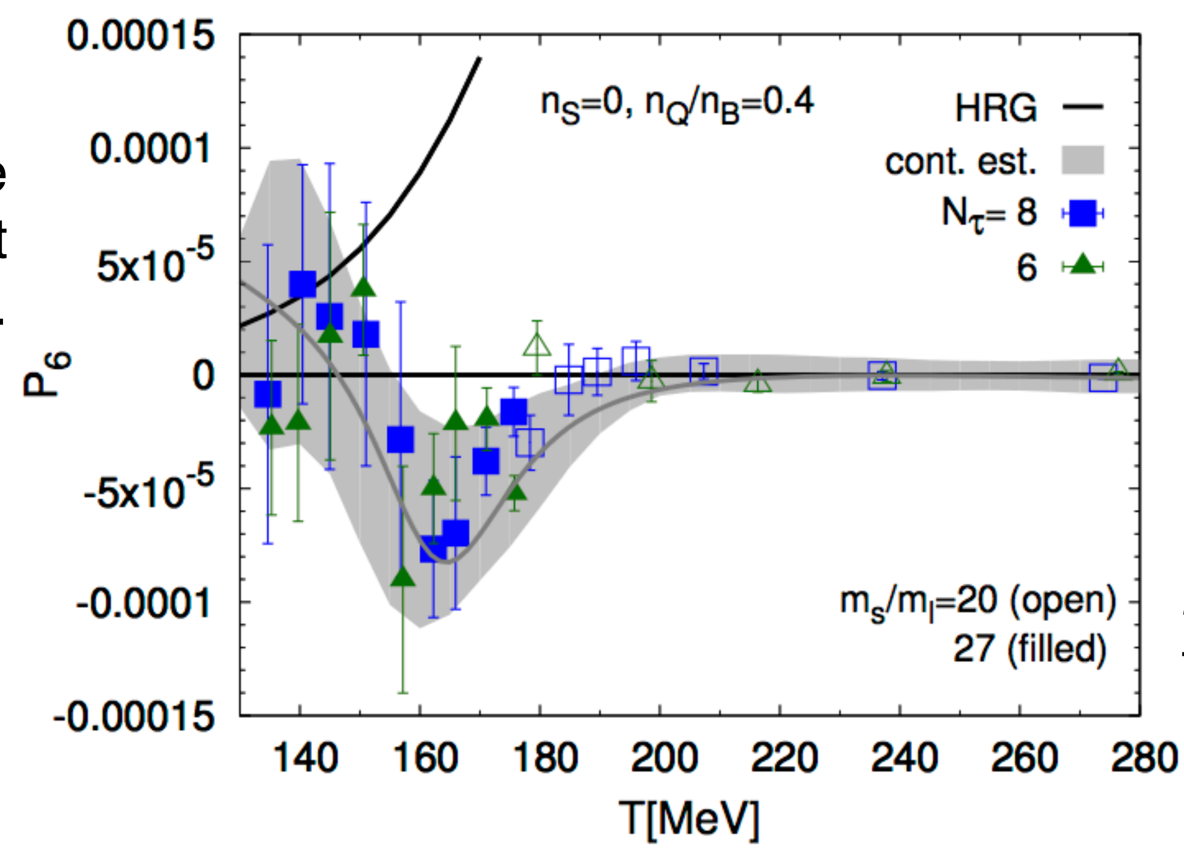

BNL-Bielefeld-CCNU, Phys. Rev. **D86**, 054504 (2017)

Shapes can be qualitatively understood as due to the 2nd order O(4) transition in the chiral limit.

Pressure, energy and entropy

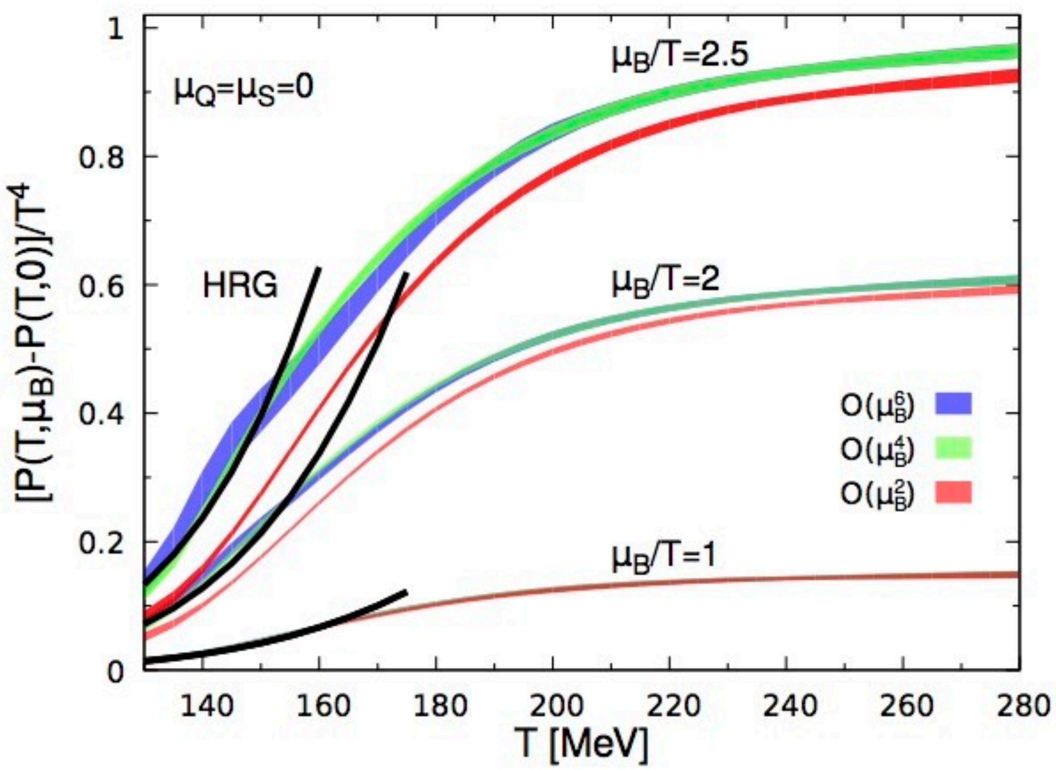

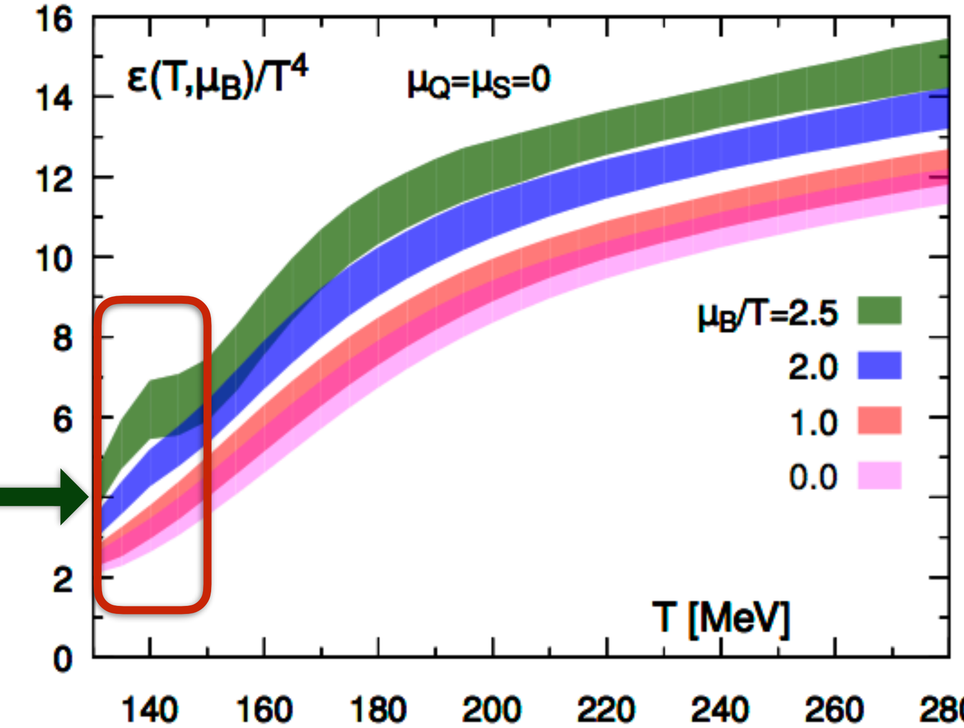

6th-order contributions start to become visible beyond $\mu_B/T = 2$

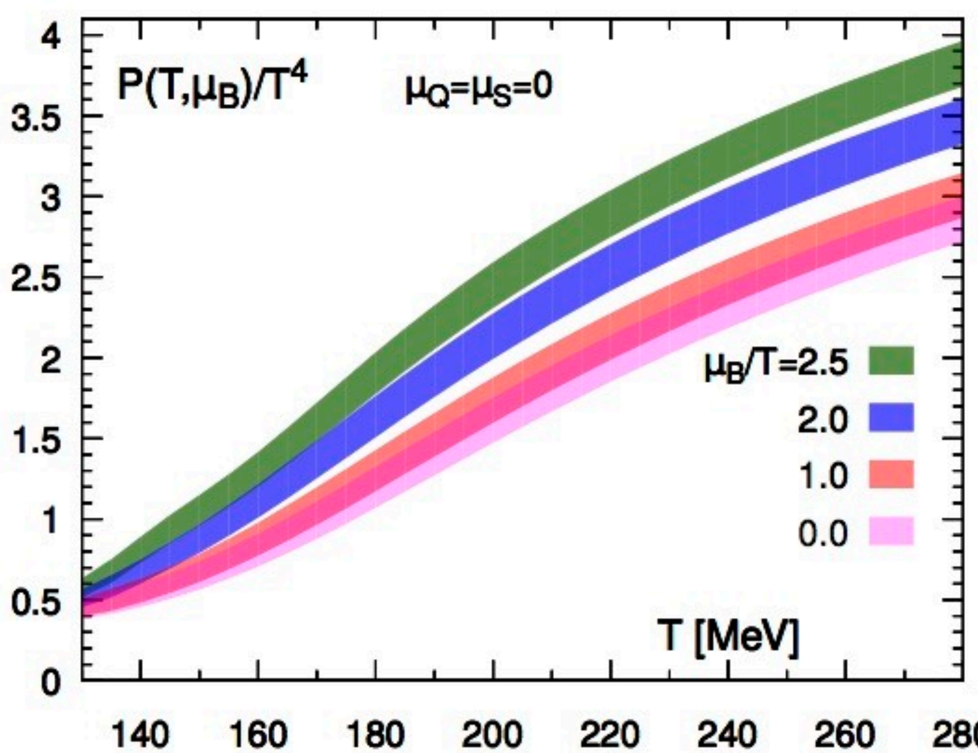

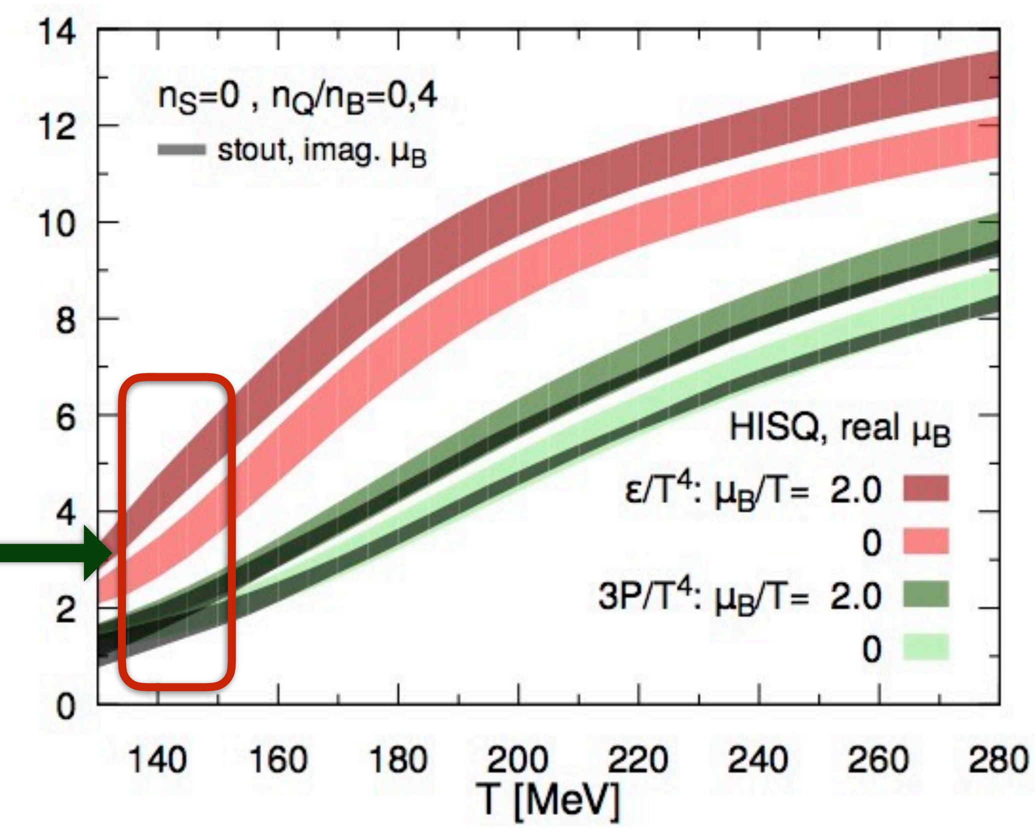

Pressure, energy and entropy

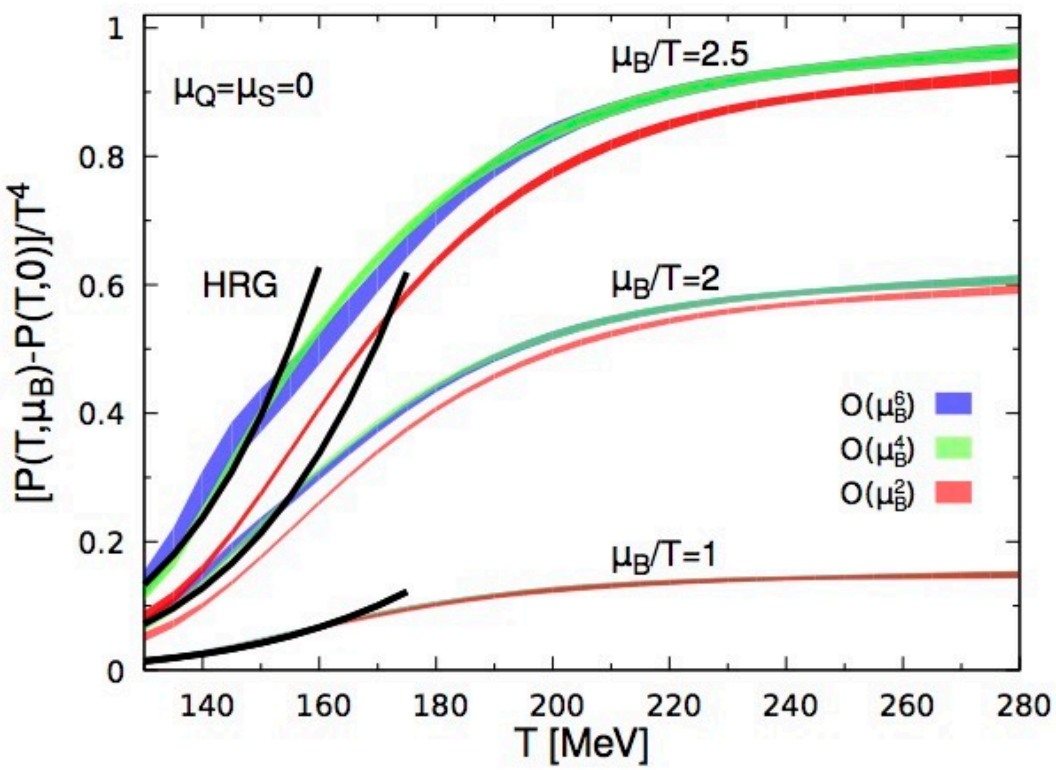

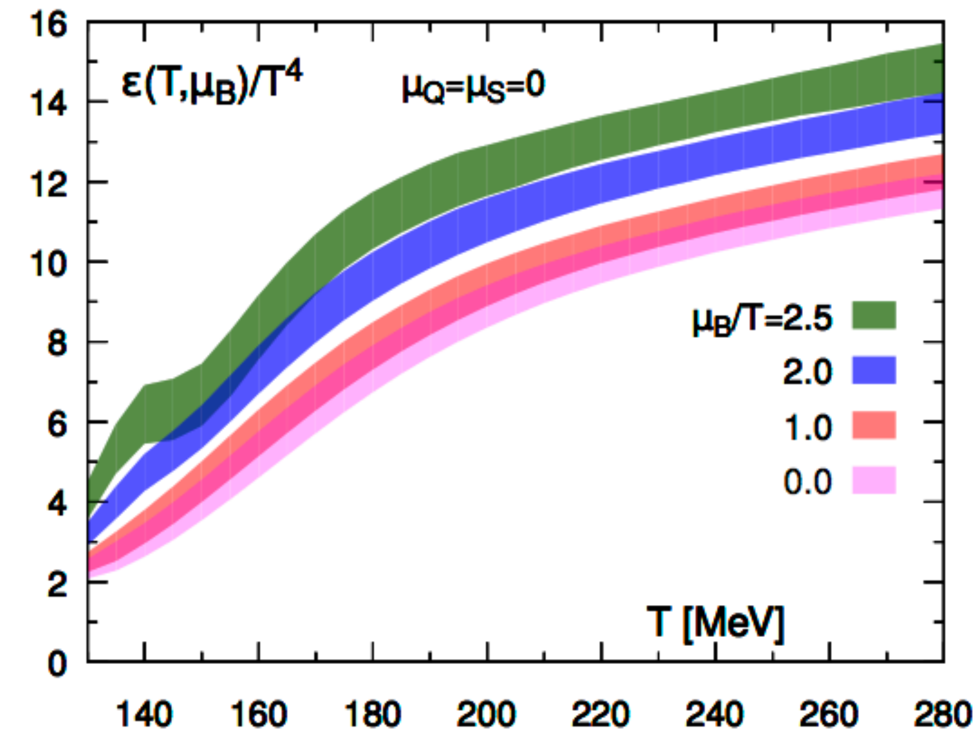

However, BES will attain chemical potentials $\mu_B/T \sim 3$ - 3.5. Clearly an 8[th] order expansion is needed (Work in progress)!

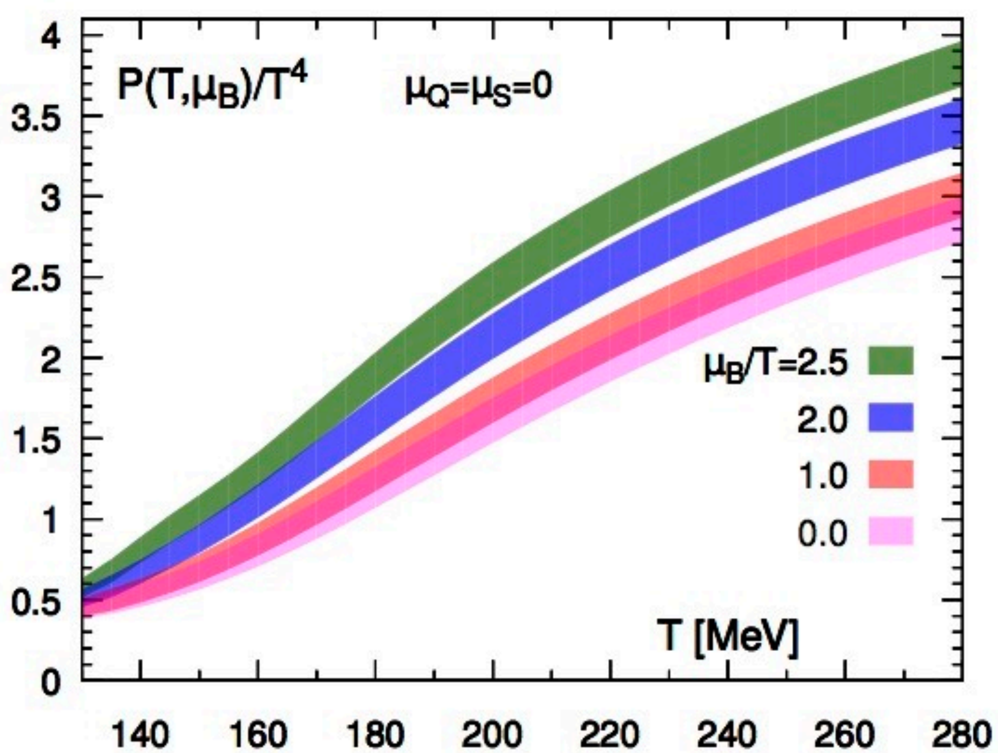

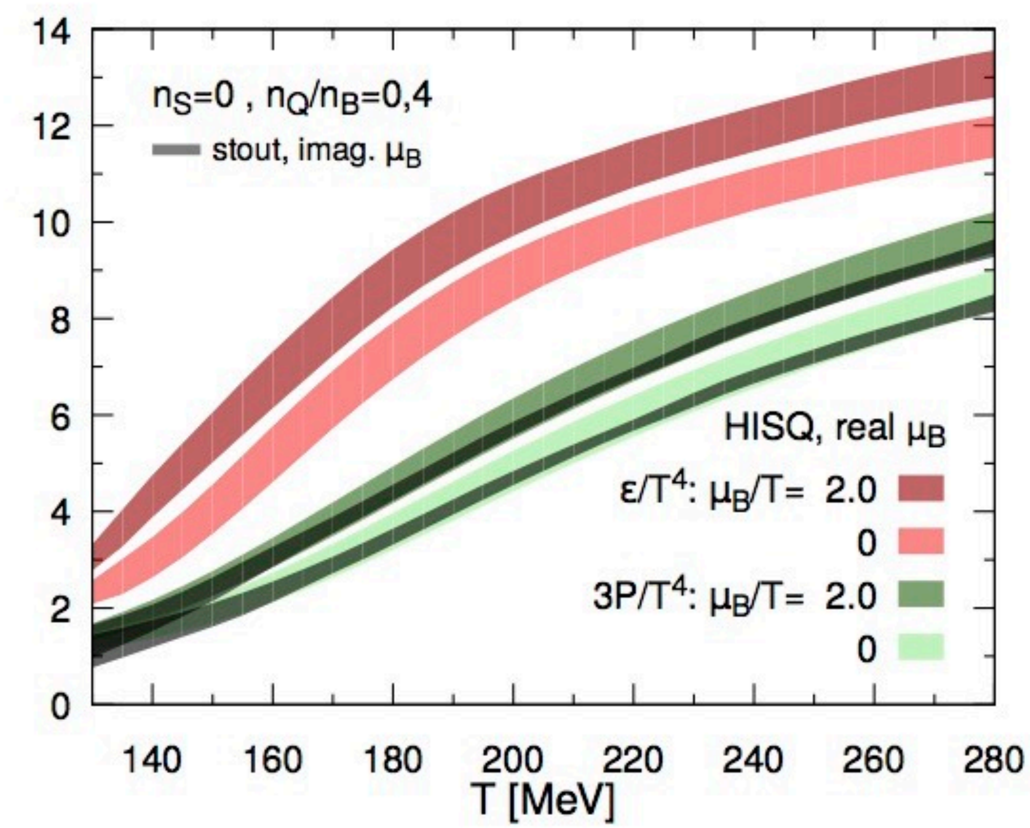

Lines of constant physics and the curvature of the freeze-out line

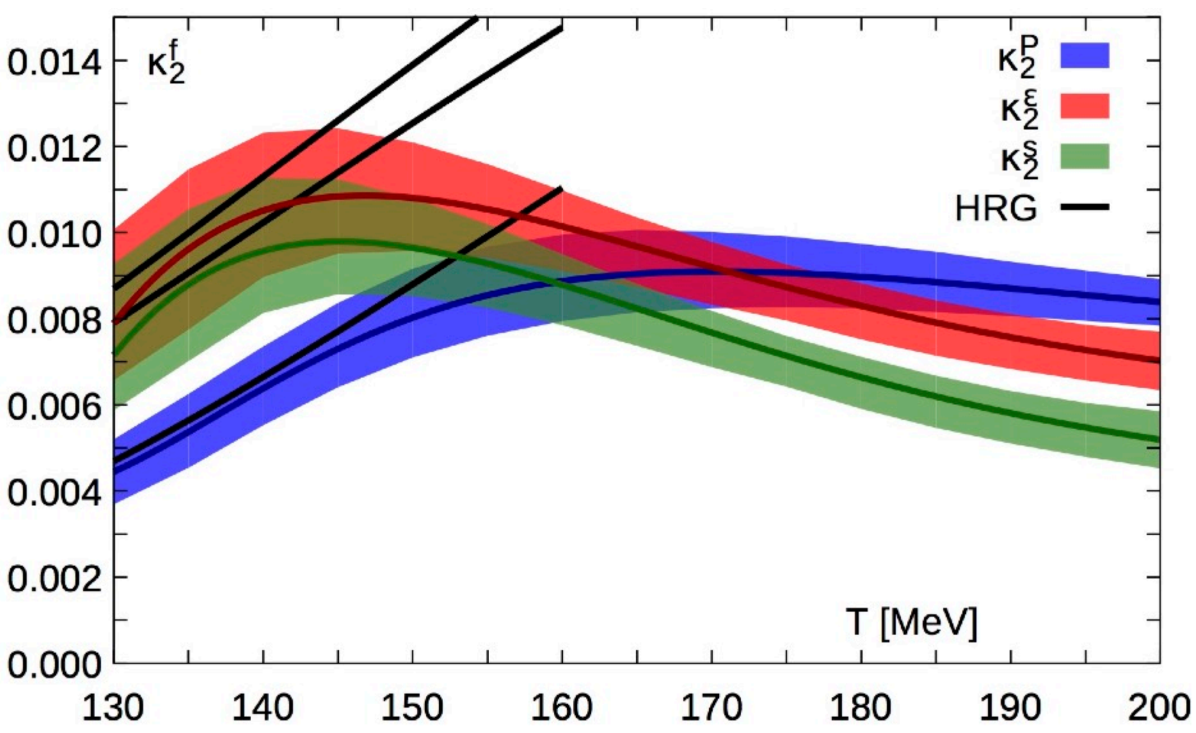

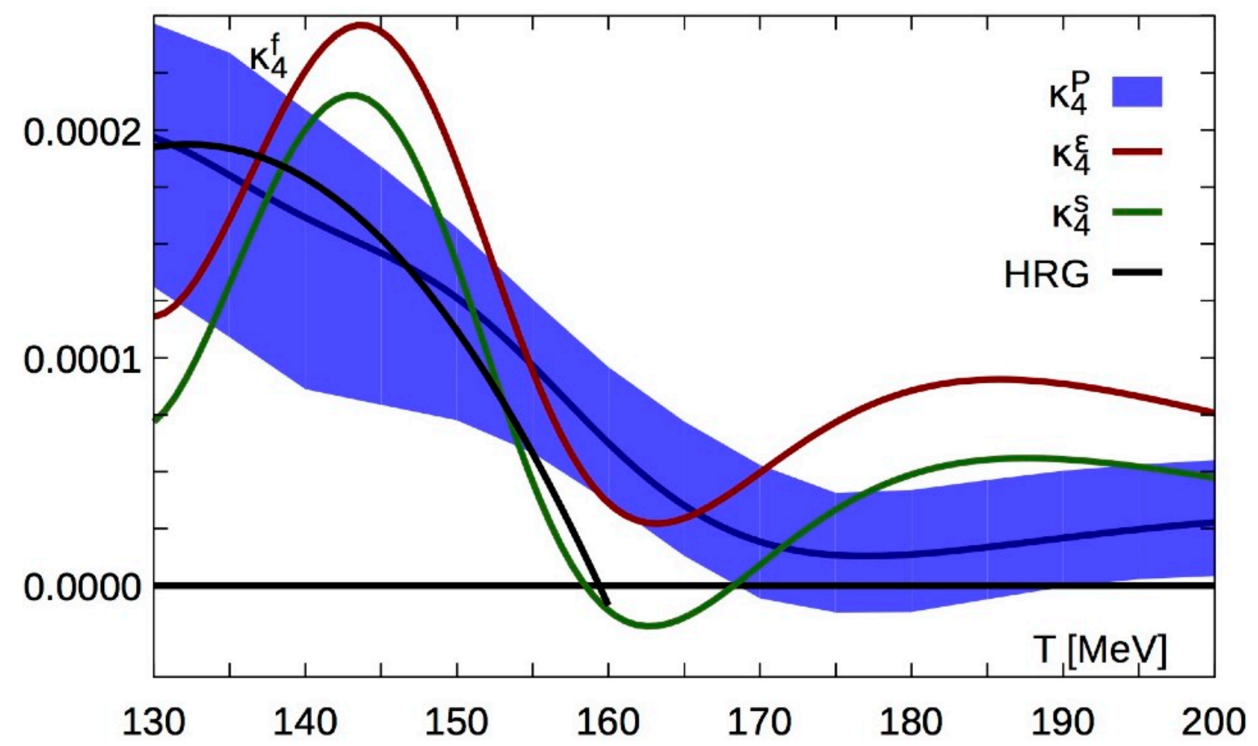

Lines of constant p, σ or ε are curves in the T-μ_B plane. For small μ_B, we can parametrize: $T(\mu_B) = T_0 + \kappa_2(\mu_B/T)^2 + \kappa_4(\mu_B/T)^4 + \ldots$

We determine κ_2 and κ_4 from our 2nd and 4th-order Taylor expansions. κ_4 is smaller than κ_2 by an order of magnitude. Our current statistics do not permit an accurate determination of κ_6.

Lines of constant physics and the curvature of the freeze-out line

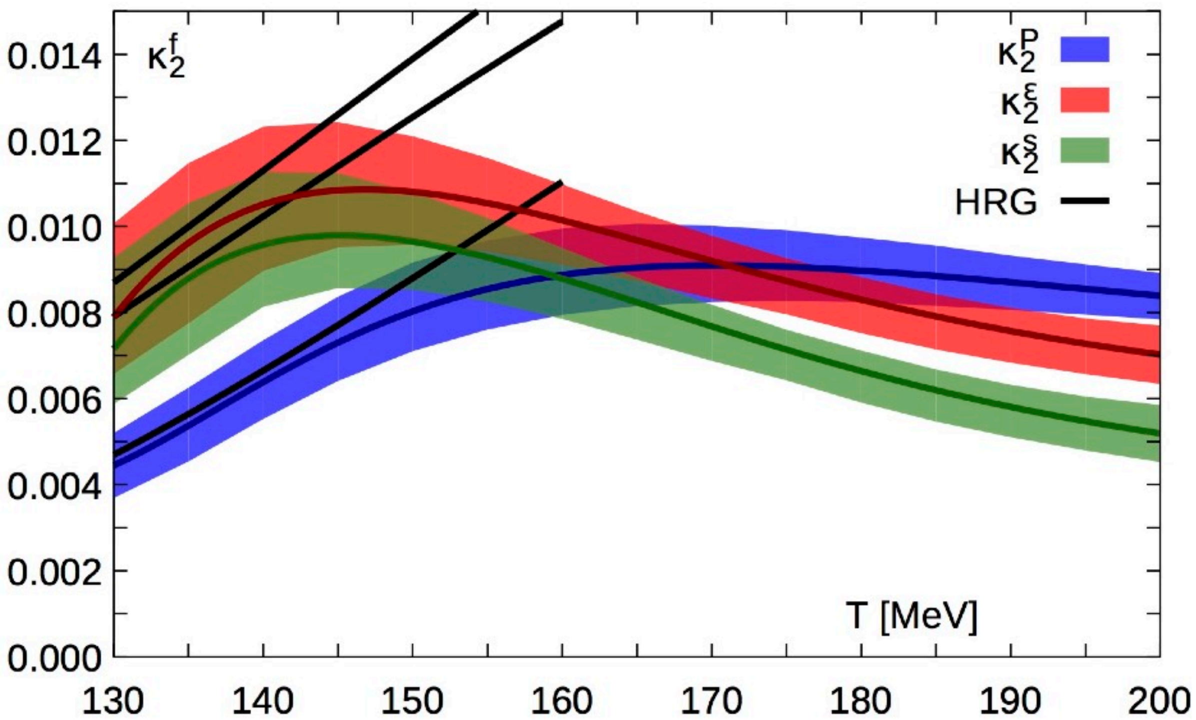

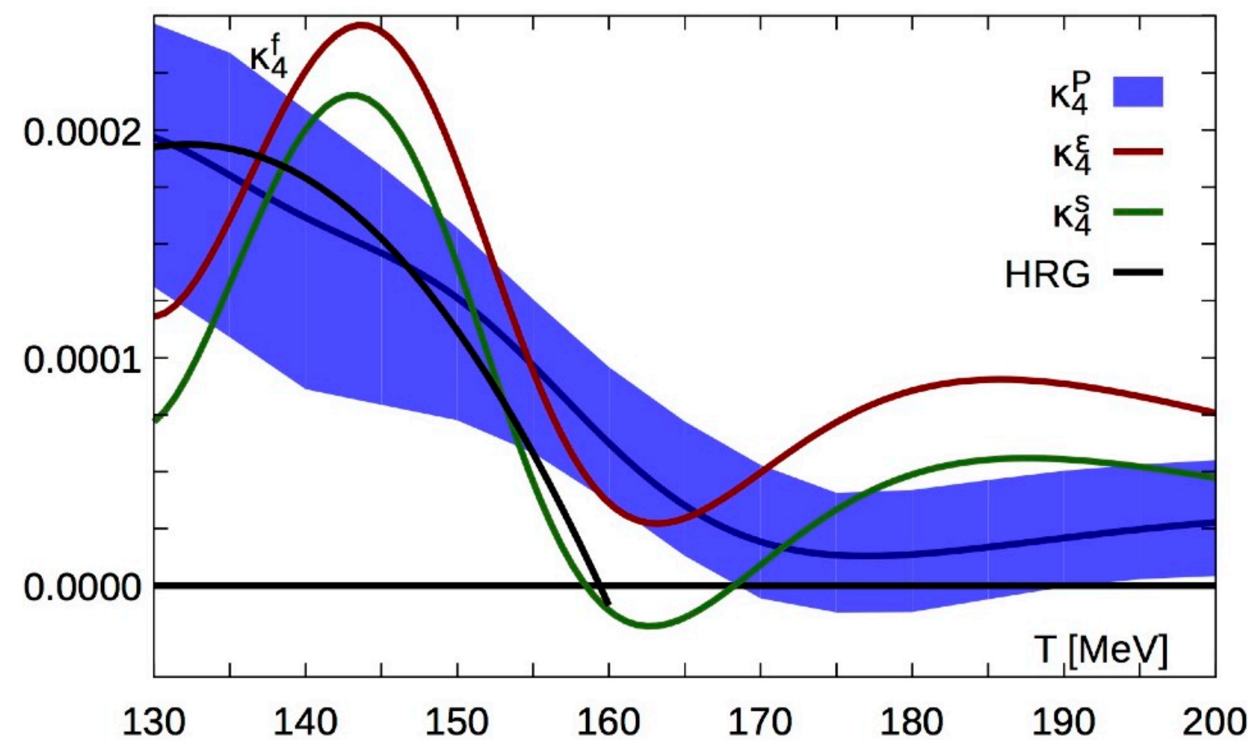

Phenomenologically, freeze-out has been conjectured to occur along such lines of constant ε or σ [Cleymans and Redlich 1999].

For T between 145 and 165 MeV, $0.0064 <= \kappa_2^p <= 0.0101$ and $0.0087 <= \kappa_2^\varepsilon <= 0.012$ [S. Sharma, QM2017]. This is in agreement with estimates for the curvature of the line of the chiral transition temperature [BNL-Bielefeld 2010; BW 2012, 2015; D'Elia *et al*. 2015; Cea *et al*. 2015].

Conclusions

- Unlike QCD at finite temperature, which by now has been fairly well-studied, the study of QCD at finite density is only just beginning.

- Lattice QCD, which works so well at finite T, unfortunately breaks down at μ not equal to 0.

- Because of this, currently one has to rely on a combination of approaches, each of which may apply to a different region of the phase diagram.

- Lattice QCD itself may be extended to the region of high T and small μ. Although only a small region of the phase diagram, this is very important as this is the region accessed in heavy-ion collisions.

- Here two approaches viz. imaginary μ and the method of Taylor expansions have met with some success. Both are computationally intensive and work in progress. Of these, the method of Taylor expansions has been successful in providing a reliable equation of state down to beam energies of ~ 12 GeV. It is hoped to extend this to cover the whole range of (T,μ) studied both at RHIC as well as at FAIR, NICA, J-PARC, etc. in the future.